Available online at www.sciencedirect.com
SCIENCE DIRECT
Precambrian Research 148 (2006) 145–180
Precambrian Research
www.elsevier.com/locate/precamres

# Carbon isotope record for the onset of the Lomagundi carbon isotope excursion in the Great Lakes area, North America

A. Bekker [a,*], J.A. Karhu [b], A.J. Kaufman [c]

[a] *Geophysical Laboratory, Carnegie Institution of Washington, 5251 Broad Branch Rd., N.W., Washington, DC 20015, USA*
[b] *Department of Geology, University of Helsinki, Helsinki FIN-00014, Finland*
[c] *Department of Geology, University of Maryland at College Park, College Park, MD 20742, USA*

Received 13 November 2005; received in revised form 16 March 2006; accepted 25 March 2006

**Abstract**

Carbonate units of the Chocolay Group in the Lake Superior area, USA and the Gordon Lake Formation of the correlative upper Huronian Supergroup, Ontario, Canada were deposited after the last Paleoproterozoic glacial event and an episode of intense chemical weathering. The Huronian Supergroup contains at the base ~2.45 Ga volcanics and is intruded by the 2.22 Ga Nipissing diabase dykes and sills while the Chocolay Group is bracketed in age between ~2.29 and 2.20 Ga. The Lomagundi (~2.22–2.1 Ga) carbon isotope excursion started after the Paleoproterozoic glacial epoch and before a plume breakout event at 2.22 Ga. Therefore, the Chocolay and Upper Huronian carbonates were deposited either before or during the onset of the Lomagundi event. Notably, thin carbonates of the basal Gordon Lake Formation and thick carbonate succession of the Kona Dolomite in the northeastern exposures of the Chocolay Group record $\delta^{13}C$ values as high as +9.5‰ versus V-PDB. Similar to other successions deposited during the Lomagundi event, both units contain pseudomorphs and molds after sulfates. This observation suggests that seawater sulfate contents rose dramatically in association with the onset of the Lomagundi event and the rise of atmospheric oxygen. Carbonates in the western and southern exposures of the Chocolay Group (Randville and Bad River dolomites, and Saunders Formation) previously assumed to be equivalent to the Gordon Lake Formation and Kona Dolomite have carbon isotope values close to 0‰. Based on basin analysis, we infer that these carbonate units were deposited during a negative carbon isotope excursion after the Lomagundi event started and are slightly younger than the Kona Dolomite and Gordon Lake Formation. This interpretation implies that the carbonate platform in the Great Lakes area transgressed to the west over shallow-marine and fluvial deposits. The negative carbon isotope excursion in the Lake Superior area might correspond to similar $\delta^{13}C$ values of the Mooidraai Dolomite in the Griqualand West Basin, South Africa supporting correlation between Paleoproterozoic successions of North America and South Africa and the notion of three global glaciations in the Paleoproterozoic Era. Carbonates of the Mille Lacs Group (Trout Lake, Glen Township, and Denham formations) in Minnesota have $\delta^{13}C$ values ranging from −1.2 to +2.5‰. Combined with geochronologic constraints, these data suggest that these units were deposited after the Lomagundi excursion and are related to the rifting event that led to development of the so far unrecognized ~2.0 Ga passive margin in the Lake Superior area.


*Keywords:* Chemostratigraphy; Basin analysis; Paleoproterozoic Era; Chocolay Group; Huronian Supergroup; Glaciation

## 1. Introduction

Progress over the last decade has significantly improved our understanding of tectonic, environmental, and climatic changes in the early Paleoprotero-

* Corresponding author. Tel.: +1 202 478 7974; fax: +1 202 478 8901.
*E-mail address:* a.bekker@gl.ciw.edu (A. Bekker).

0301-9268/$ – see front matter © 2006 Elsevier B.V. All rights reserved.
doi:10.1016/j.precamres.2006.03.008

zoic Era. Assembly of the supercontinent Kenorland in the Late Archean up to ~2.42 Ga time interval overlapped with plume breakout events between 2.48 and 2.42 Ga (Barley et al., 2005), and was closely followed by three global glaciations (Young, 2002). Associated with these three ice ages are two strongly positive carbon isotope excursions; one is arguably bracketed between the second and the last glacial events and called the Duitschland event, and the other radiometrically constrained between 2.22 and 2.06 Ga and named the Lomagundi event follows the glacial epoch. While the older excursion is confined to the Duitschland Formation of South Africa (Bekker et al., 2001) and has not yet reproduced in other basins potentially due to the lack of carbonates in a correlative stratigraphic position, the younger event is recognized in a number of basins worldwide and has proven useful for interbasinal correlation (cf. Karhu and Holland, 1996; Bekker et al., 2003). Geochemical and lithologic evidence for the rise of atmospheric oxygen level occur stratigraphically below the Lomagundi excursion, and perhaps beneath the older excursion as well (Bekker et al., 2005).

The duration and amplitude of the Lomagundi excursion is striking and finds no match in Earth history. It has been argued that this apparently long-lived event may have included several oscillatory sub-cycles (Melezhik et al., 1999). Our earlier review of available age constraints (Bekker et al., 2003a), however, supported the more conservative view of a single sustained event. The issue is complicated by the general absence of carbonates above the last Paleoproterozoic glacial diamictite. Instead, this post-glacial time interval appears to be one of global deposition of mature quartz sandstones and rare evaporites, suggesting extreme greenhouse conditions. Thin carbonates are rarely present within these mature quartz sandstones. These carbonates have highly variable $\delta^{13}C$ values ranging from 0 to +5‰ versus V-PDB (Lower Jatulian Group, Karelia and Kola Peninsula, Russia: Yudovich et al., 1990; Tikhomirova and Makarikhin, 1993; Melezhik and Fallick, 1996; Magusa and Whiterock members of the Kinga Formation, Hurwitz Group, Nunavut, Canada: Bekker et al., unpublished; Cercadinho Formation, Minas Supergroup, Brazil: Bekker et al., 2003).

To further investigate this post-glacial time interval, we present a chemostratigraphic and basin analysis of carbonates from the Gordon Lake Formation in the Upper Huronian Supergroup of Canada, which is younger than the ultimate Paleoproterozoic glacial event and intruded by the 2.22 Ga Nipissing diabase dykes and sills, as well as carbonates from broadly correlative units of the Chocolay Group in Wisconsin and Michigan and the Mille Lacs Group of Minnesota. Our objectives are (1) to use carbon isotope data as a test of lithostratigraphic correlations in the region; (2) to provide new constraints for development of Paleoproterozoic basins in the Great Lakes area; and (3) to characterize the tempo and mode of carbon isotope variations of the ocean in the aftermath of the Paleoproterozoic glacial epoch and through the Lomagundi event.

## 2. Regional setting and stratigraphy

Early Paleoproterozoic successions preserved along the southern margin of the Superior Craton include thick, predominantly siliciclastic packages. The Huronian Supergroup outcrops along the north shore of Lake Huron, Ontario, Canada and in a series of large outliers to the east-northeast of Lake Huron (Young, 1991; Fig. 1). The lower part of the Huronian Supergroup was deposited in a rift setting, while the upper part (starting with the Gowganda Formation; see Fig. 2) is a passive margin succession dominated by siliciclastic sediments (Zolnai et al., 1984; Young et al., 2001). The Huronian Supergroup is subdivided by unconformities into four groups, the upper three are climatically controlled cycles with glacial diamictites at the base followed by deltaic mudstones or carbonate and overlain by thick fluvial sandstones (Young et al., 2001).

The basal Huronian rests unconformably with locally preserved reduced paleosols on the Archean Superior Province (Prasad and Roscoe, 1996) and contains conglomerates with detrital pyrite and uraninite of the Livingstone Creek and Matinenda formations, suggesting low atmospheric oxygen content during their deposition. Interlayered volcanic rocks and intrusive contacts with the Murray and Creighton granites constrain the age of the basal Huronian to 2.48–2.42 Ga (Krogh et al., 1984, 1996; Smith and Heaman, 1999; Smith, 2002), while the entire Huronian Supergroup was folded and subsequently intruded by the $2217.5 \pm 1.6$ Ma Nipissing sills and dykes (Andrews et al., 1986). Facies change dramatically across the latitudinal Murray Tectonic Zone that separates shallow water sequences with subgreenschist to lower greenschist facies of metamorphism and open folds to the north from deeper water, thicker sequences with higher metamorphic grade and tight upright folds to the south (Card, 1978). Paleocurrent indicators in the lower Huronian sandstones, facies analysis, and isopach maps suggest a paleoslope towards the southeast (Fralick and Miall, 1989; Rousell and Long, 1998).

The upper part of the Huronian Supergroup deposited above the youngest Paleoproterozoic glacial deposit con-

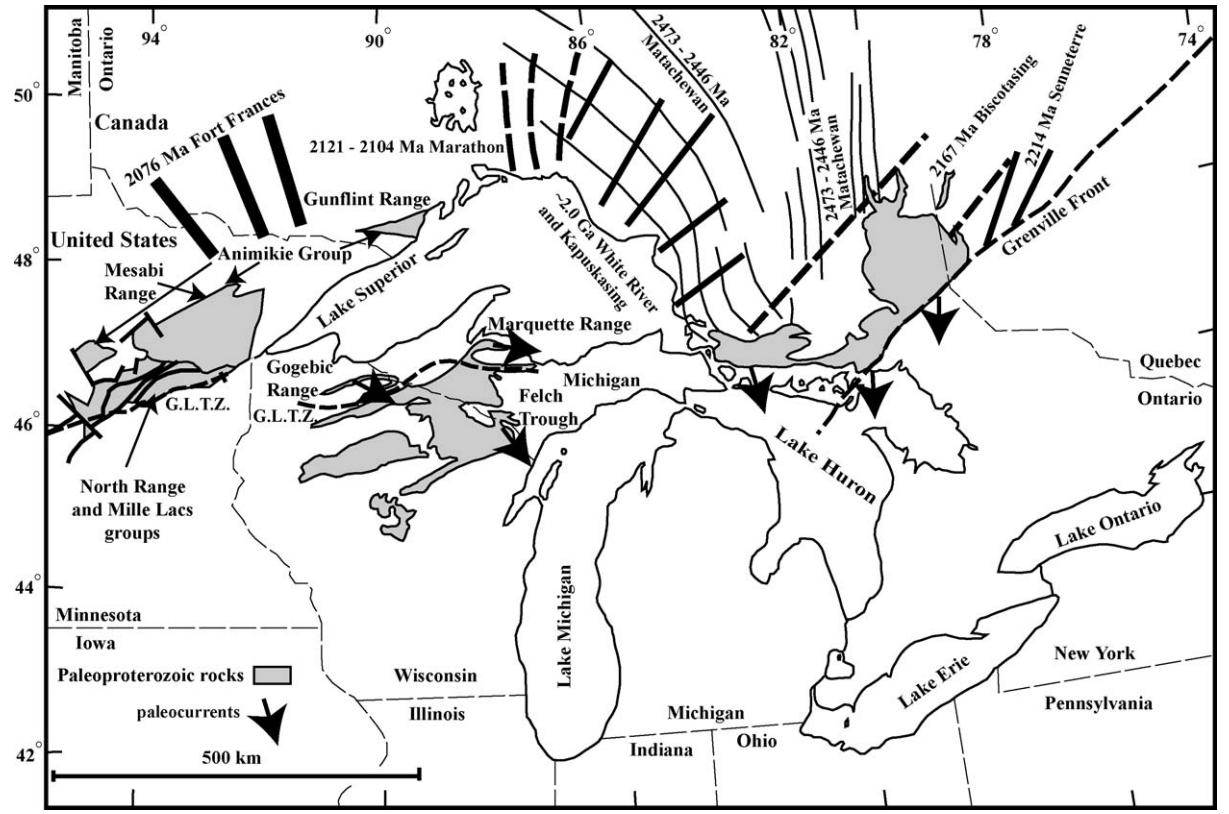


Fig. 1. Geological map of the Great Lakes area showing Paleoproterozoic successions (modified from Young, 1983; Morey, 1996; Ojakangas et al., 2001). Paleocurrents data are from Larue (1979, 1981), Long (2004), Pettijohn (1957) and Rousell and Long (1998) and dyke swarms from Halls and Davis (2004). G.L.T.Z. is Great Lakes Tectonic Zone.

tains deltaic mudstones and sandstones of the upper Gowganda Formation overlain by mature quartzites of the fluvial Lorrain and tidally-influenced Bar River formations separated by a thinly interbedded succession of varicolored and silicified mudstone, siltstone, sandstone, and rare carbonate of the Gordon Lake Formation. While unaltered feldspar grains are present in the lower part of the Lorrain Formation, these are lacking in the middle and upper parts of the unit where pyrophyllite, sericite, kaolinite, and diaspore represent products of deep weathering in a warm and humid climate (Wood, 1973; Chandler, 1984). Carbonates occur locally in the shallow subtidal storm-influenced Gordon Lake Formation (Hofmann et al., 1980; Bennett et al., 1991; Jackson, 1994). The upper part of the Huronian Supergroup provides evidence for an oxygenated atmosphere including red beds (Wood, 1979; Young et al., 2001), an oxidized Ville Marie paleosol below the Lorrain Formation (Rainbird et al., 1990; Panahi et al., 2000), and pseudomorphs after anhydrite in the Gordon Lake Formation (Chandler, 1988) consistent with an intensification of the oxidative sulfur cycle. Aluminum-rich and mature quartzites in the middle and upper parts of the Lorrain Formation imply climatic amelioration in the aftermath of the glaciation (Wood, 1973; Long et al., 1999).

The upper part of the Huronian Supergroup has been considered to be lithostratigraphically correlative with the Chocolay Group of the Marquette Range Supergroup, which outcrops along the southern shore of the Lake Superior in Michigan and Wisconsin, USA. The Chocolay Group was likely deposited in a failed rift basin extending to the west from the open continental margin where the upper part of the Huronian Supergroup accumulated (Young, 1983). Diamictites of the Gowganda, Enchantment Lake, and Fern Creek formations and mature quartzites and Al-rich fine-grained rocks of the Lorrain Formation, Sturgeon River, Mesnard, and Sunday Quartzites have been correlated (Young, 1983; Ojakangas et al., 2001; Argast, 2002; Fig. 2). However, glacial diamictites are confined to the eastern part of the Chocolay Group outcrop area in the Upper Peninsula of Michigan beneath the studied Kona and Randville Dolomites, to the west and south where other carbonates were

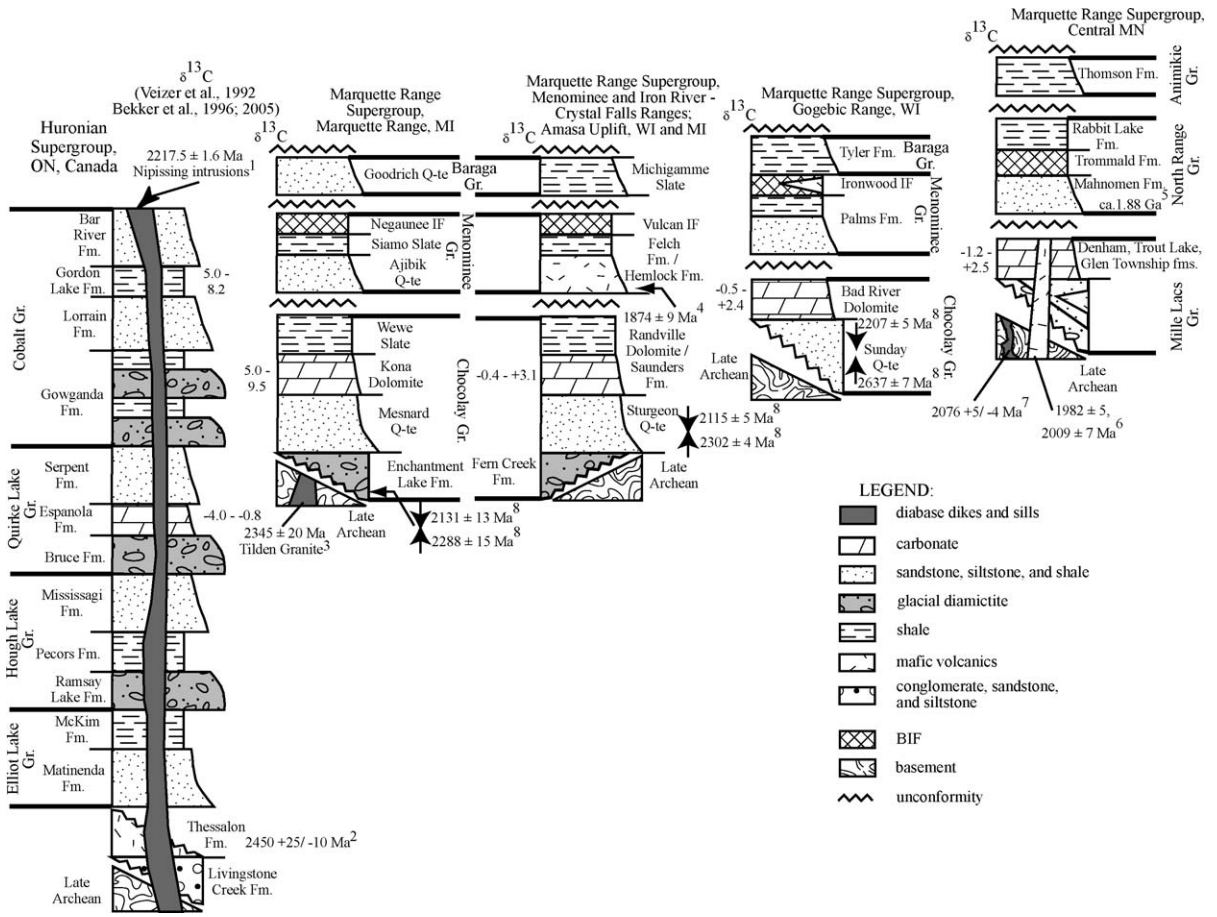


Fig. 2. Correlation of the Paleoproterozoic successions of the Great Lakes area. References to age constraints—1: Andrews et al. (1986); 2: Krogh et al. (1984); 3: Hammond (1976); 4: Schneider et al. (2002); 5: Vallini et al. (2003); 6: Goldich and Fischer (1986), Holm et al. (2005); 7: Buchan et al. (1996); 8: Vallini et al. (2005, in press). Age with an arrow pointing up indicates detrital zircon age (maximum age of deposition); age with an arrow pointing down indicates hydrothermal xenotime age (minimum age of deposition). Carbon isotope data are from this study unless otherwise stated.

investigated mature quartzites unconformably overlie Archean basement. The absence of glacial diamictites in the latter areas may be related to erosion prior to the deposition of the mature quartzites (Morey and Southwick, 1995) as reflected elsewhere by thick sericitic schist between glacial diamictite and overlying mature quartzites interpreted as reworked aluminum-rich regolith (Ojakangas, 1997; LaBerge et al., 2003).

Chocolay quartzites are up to 600 m thick, contain redbeds and were deposited in a tidally-influenced shallow-marine environment (Larue, 1981). Carbonates of the Chocolay Group (Randville, Kona, and Bad River Dolomites, and Saunders Formation) conformably overlie the mature quartzites and may be broadly correlative with the Gordon Lake Formation of the Huronian Supergroup (Young, 1983; Bennett et al., 1989). Accepting that these carbonates belong to the same basin, differences in facies and the lack of independent evidence for age equivalence alternatively suggests that these units may have been deposited at slightly different times (Van Hise and Bayley, 1897; Tyler and Twenhofel, 1952). The Chocolay carbonates are unconformably overlain by the ~1.88 Ga Menominee Group deposited in the back-arc basin (Fralick et al., 2002), except the Marquette Trough area where the Wewe Slate deposited below wave base sit between the unconformity and the Kona Dolomite (Larue, 1981).

The Mille Lacs Group of north-central Minnesota contains carbonates of the Trout Lake, Glen Township, and Denham formations. The succession is considered broadly correlative with the Chocolay Group and the Gordon Lake Formation of the Upper Huronian Supergroup (Larue, 1981; Sims et al., 1981; Morey and

Southwick, 1995). However, neither glacial diamictite nor mature quartzite are present in this unit, which is confined to the offset in the Great Lakes Tectonic Zone (G.L.T.Z.; see Fig. 1), a major Late Archean suture (Sims et al., 1980).

New SHRIMP U–Pb ages of detrital zircons and hydrothermal xenotimes from the Chocolay Group bracket the depositional age of this group and, consequently, the age of the last Paleoproterozoic glaciation between 2288 ± 15 and 2207 ± 5 Ma (Vallini et al., in press). The Tilden granite cutting the Archean Compeau Gneiss near Marquette, Upper Peninsula of Michigan may be related to rifting and initiation of the Chocolay Basin insofar as it yielded TIMS U–Pb zircon age of 2345 ± 20 Ma (Hammond, 1976). Since all these carbonate units are younger than the Paleoproterozoic glacial epoch, we adopt ~2.30 Ga as their maximum age.

## 3. Analytical methods

The carbonate-rich sections were measured and samples were collected from fresh carbonate intervals lacking shear, foliation, or fractures. Samples collected for whole rock analyses were cleaned, cut, and powdered; these are marked with a dollar sign in Table 1. Other samples were petrographically characterized and least altered (lacking veins, discoloration, weathering rinds, and silicification) and finest-grained portions of polished thick sections were microdrilled with 1 mm diamond drill. Thin sections contain xenotopic mosaics of anhedral, coarsely crystalline to very coarsely crystalline dolomite crystals with pseudospar and veins and fractures filled with quartz, very coarsely crystalline carbonate and muscovite. While micrite and spar did not survive through neomorphism and recrystallization during diagenesis and metamorphism, gross primary textures (e.g. laminations) are still present. Manganese, Sr, and Fe concentrations and C, O, and Sr isotopic measurements were completed and quantified using procedures outlined in detail by Bekker et al. (2003).

Sulfur isotope composition of barites was measured at the University of Maryland by continuous flow mass spectrometry following the method of Grassineau et al. (2001). A Eurovector elemental analyzer was used for on-line combustion of sulfate samples and $SO_2$ separation and delivery to a Micromass IsoPrime mass spectrometer for $^{34}S/^{32}S$ analyses. Isotopic results are expressed in the $\delta$ notation as per mil (‰) deviations from the Vienna-Canyon Diablo troilite (V-CDT) standard. Based on multiple analyses of standard materials the uncertainty of measurements ($1\sigma$) is typically 0.3‰ or less.

## 4. Studied sections and geochemical results

### 4.1. Gordon Lake Formation, Upper Huronian Supergroup, Ontario, Canada

The >2.22 Ga Gordon Lake Formation is 300–700 m thick and consists of well-bedded, variegated mudstone and siltstone; chert; and minor fine-grained quartz sandstone that contains rare beds and nodules of dolomite (Hofmann et al., 1980; Bennett et al., 1991; Young, 1991; Jackson, 1994). The unit is subdivided into three members: a lower member consisting of red sandstone and siltstone with chert and anhydrite/gypsum nodules (Chandler, 1988); a middle member composed of green siltstone and mudstone with minor sandstone; and an upper member made up of red siltstone, mudstone, and chert. Chamosite and glauconite are present in the middle part of the formation indicating marine environment (Wood, 1973; Chandler, 1986). The lower part of the formation was deposited in a sabkha tidal-flat setting; the middle part represents transgressive storm-influenced marine environment below tidal current influence; and the upper part is the regressive section grading towards tidal-flat setting of the overlying Bar River Formation (Chandler, 1986). The lower part of the formation includes stratiform copper mineralization likely derived by continental brines from underlying red beds (Pearson, 1979; Chandler, 1989). Anhydrite nodules in the lower Gordon Lake Formation have $\delta^{34}S$ values ranging from +12.3 to +15.6‰ versus CDT likely reflecting seawater composition at that time (Cameron, 1983). Carbonates of the Gordon Lake Formation are restricted to the base of the formation and occur in several localities (Fig. 3) as thin laminated dolostone beds with fenestral fabrics (Plummer Township; Hofmann et al., 1980), siliceous dolostone-bearing beds and dolostone nodules (Meredith and Johnson townships; Jackson, 1994), and impure dolomite beds (Welcome Lake of the Cobalt area; Chandler, 1986). Bennett et al. (1989) described a finely laminated to massive dolostone unit in a fault-bounded block in Fenwick Township, Goulais Bay area about 27 km north of Sault Ste. Marie and correlated it with the Gordon Lake Formation. The most extensive outcrop of the dolostone unit consists of pink dolomicrite; pale-grey doloarenite with quartz grains, oölites, intraformational flat-pebble conglomerate, and stratiform copper deposit; 20–30 cm thick lenses of pale-pink to grey barite; and chert (Bennett et al., 1989). The carbonate unit is at least 30 m thick (Bennett et al., 1989). The base of the section consists of grey-maroon shale interlayered with dolomite, thin layers of sandstone occur in the lower and middle parts of the section, and carbonates

Table 1
Results of chemical and isotopic analyses

| Sample # | Analyzed mineral/rock | $\delta^{13}C_{carb}$ (‰, V-PDB) | $\delta^{18}O_{carb}$ (‰, V-PDB) | TOC (mg C/g sample) | $\delta^{13}C_{org}$ | $\Delta^{13}C_{carb-org}$ | Fe (%) | Mn (ppm) | Sr (ppm) | Mn/Sr | $^{87}Sr/^{86}Sr$ |
|---|---|---|---|---|---|---|---|---|---|---|---|
| Gordon Lake Formation | | | | | | | | | | | |
| Fenwick Township (46°45′51″N, 84°27′30″W) | | | | | | | | | | | |
| KN-1$ | Dolomite | 7.2 | −12.3 | | | | 0.98 | 1568 | 177 | 8.9 | |
| KN-2$ | Dolomite | 7.3 | −13.4 | | | | 0.51 | 945 | 149 | 6.3 | |
| KN-3$ | Dolomite | 6.4 | −12.8 | | | | 1.04 | 1193 | 173 | 6.9 | |
| KN-4$ | Dolomite | 6.9 | −11.8 | | | | 1.04 | 2052 | 206 | 9.9 | |
| KN-5$ | Dolomite | 8.2 | −10.3 | | | | 0.33 | 694 | 151 | 4.6 | |
| KN-6$ | Dolomite | 5.0 | −14.8 | | | | 0.60 | 1277 | 73 | 17.4 | |
| GO-1-3$ | Dolomite | 5.0 | −16.6 | | | | | | | | |
| GO-1-4$ | Dolomite | 6.2 | −14.7 | | | | 0.87 | 1205 | 199 | 6.0 | |
| GO-1-6$ | Dolomite | 5.8 | −12.9 | | | | | | | | |
| GO-1-10$ | Dolomite | 8.0 | −11.3 | | | | 0.45 | 507 | 151 | 3.4 | |
| GO-1-11$ | Dolomite | 7.7 | −12.7 | | | | 0.34 | 524 | 144 | 3.7 | |
| GO-1-12$ | Dolomite | 7.1 | −13.6 | | | | | | | | |
| GO-1-13$ | Dolomite | 7.6 | −12.0 | | | | | | | | |
| GO-1-14$ | Dolomite | 8.2 | −9.9 | | | | | | | | |
| Fe-3* | Dolomite | 2.1 | −16.2 | | | | | 3979 | 202 | 19.7 | |
| Plummer Township (46°23′57″N, 83°48′00″W) | | | | | | | | | | | |
| GO-4-1$ | Dolomite | 5.7 | −12.7 | | | | 0.90 | 6803 | 95 | 71.9 | |
| GO-4-2$ | Dolomite | 5.9 | −11.9 | | | | 0.66 | 5899 | 93 | 63.5 | |
| GO-4-3$ | Dolomite | 5.6 | −13.2 | | | | | | | | |
| GO-4-4$ | Dolomite | 5.5 | −13.2 | | | | | | | | |
| PL-1* | Dolomite | 5.6 | −10.5 | | | | | 4839 | tr. | – | |
| PL-2* | Dolomite | 5.8 | −10.4 | | | | | 4360 | 48 | 91.4 | |
| PL-3* | Dolomite | 5.6 | −9.9 | | | | | 3617 | 70 | 51.5 | |
| PL-4* | Dolomite | 5.5 | −10.4 | | | | | 5439 | 28 | 196.4 | |
| PL-5* | Dolomite | 5.8 | −9.4 | | | | | 2835 | tr. | – | |
| PL-5A* | Dolomite | 6.2 | −8.9 | | | | | 2733 | 22 | 123.6 | |
| PL-6* | Dolomite | 5.5 | −9.5 | | | | | 4261 | 17 | 248.3 | |
| PL-7* | Dolomite | 5.5 | −8.6 | | | | | 4577 | 151 | 30.3 | |
| Aberdeen Additional Township | | | | | | | | | | | |
| JT-1$ | Dolomite | 7.5 | −13.1 | | | | 0.77 | 7364 | 144 | 51.2 | |
| Central Meredith Township (<100 m south of HW 638, Zone 17, 273282E, 5150075N) | | | | | | | | | | | |
| GO-2-1$ | Dolomite | 2.6 | −17.6 | | | | | | | | |
| Go-2-2$ | Dolomite | 4.3 | −13.7 | | | | | | | | |
| GO-2-3$ | Dolomite | 4.2 | −13.6 | | | | 0.59 | 10594 | 79 | 134.0 | |
| GO-2-4$ | Dolomite | 3.6 | −13.7 | | | | | | | | |
| GO-2-5$ | Dolomite | 4.1 | −13.7 | | | | 0.56 | 10252 | 79 | 129.9 | |

| | | | | | | | | | | |
|---|---|---|---|---|---|---|---|---|---|---|
| GO-2-6$ | Dolomite | −1.0 | −19.6 | | | | | 9526 | 65 | 147.2 |
| JT-98-1/1* | Dolomite | 4.4 | −10.9 | | | | | 9550 | 2 | 4623.1 |
| JT-98-1/2* | Dolomite | 3.8 | −11.4 | | | | | 9607 | 20 | 491.0 |
| JT-98-1/3* | Dolomite | 3.9 | −11.3 | | | | | 11562 | 31 | 367.7 |
| JT-98-2* | Dolomite | 2.9 | −12.5 | | | | | 5968 | tr. | – |
| JT-98-3* | Dolomite | 3.4 | −14.9 | | | | | 6597 | tr. | – |
| JT-98-5/1* | Dolomite | 1.3 | −12.9 | | | | | 5927 | tr. | – |
| JT-98-5/2* | Dolomite | 4.6 | −10.1 | | | | | | | |
| Carbonate unit in the Killarney Bay Park | | | | | | | | | | |
| KB-2* | Dolomite | −8.7 | −7.9 | | | | | | | |
| KB-4* | Dolomite | 0.4 | −6.2 | | | | | 1611 | 26 | 62.9 |
| KB-5* | Dolomite | −1.5 | −7.3 | | | | | 320 | tr. | – |
| KB-6* | Dolomite | −1.9 | −7.8 | | | | | 465 | tr. | – |
| Kona Dolomite, Chocolay Group, Marquette Range Supergroup, Marquette Trough, Upper Peninsula Michigan, USA | | | | | | | | | | |
| 17072/USGS$ | Dolomite | 6.3 | −12.9 | | | | 0.27 | 3855 | 110 | 35.1 |
| HW 480, MI (SW1/4, Sec. 8, T.47N, R.25W) | | | | | | | | | | |
| 93-MI-61-B$ | Dolomite | 6.1 | −13.8 | | | | 0.26 | 526 | 258 | 2.0 |
| 93-MI-61-D$ | Dolomite | 6.1 | −13.8 | | | | 0.27 | 592 | 225 | 2.6 |
| 93-MI-61-F$ | Dolomite | 5.9 | −13.2 | | | | 0.50 | 553 | 231 | 2.4 |
| 93-MI-61-G$ | Dolomite | 6.2 | −12.5 | | | | 0.29 | 604 | 253 | 2.4 |
| Lindberg Pit, HW 480, MI (SW1/4, Sec. 8, T.47N, R.25W) | | | | | | | | | | |
| 93-MI-L$ | Dolomite | 6.0 | −13.7 | | | | 0.38 | 871 | 237 | 3.7 |
| MI-KN-1$ | Dolomite | 4.9 | −13.7 | | | | 1.49 | 1253 | 329 | 3.8 |
| MI-KN-2$ | Dolomite | 6.0 | −14.1 | | | | 0.40 | 1107 | 231 | 4.8 |
| HW 28 near Marquette State Prison, MI (NE1/4, Sec. 1, T.47N, R.25W) | | | | | | | | | | |
| MI-95-C-2$ | Dolomite | 6.9 | −12.4 | | | | 0.34 | 2216 | 141 | 15.7 |
| MI-95-C-4$ | Dolomite | 6.7 | −15.3 | | | | 0.76 | 2997 | 160 | 18.8 |
| Lower Argillite Member, NE1/4, SW1/4, Sec. 8, T.47N, R.25W, Hole 21, Depth 1222', Cliff Mining Services Company | | | | | | | | | | |
| KO-1-23$ | Dolomite | 5.5 | −17.1 | | | | 1.68 | 7799 | 296 | 26.4 |
| Mount Mesnard, MI (NW1/4, Sec. 34, T.48N, R.25W) | | | | | | | | | | |
| Lower Argillite Member | | | | | | | | | | |
| MM-1* | Argillite | | | 0.1 | −17.3 | | | | | |
| MM-2* | Argillite | | | 0.1 | −18.1 | | | | | |
| MM-4* | Argillite | | | 0.1 | −23.2 | | | | | |
| Lower Quartzite Member | | | | | | | | | | |
| MM-7* | Dolomite | 6.0 | −11.3 | | | | | 5787 | 73 | 78.9 |
| MM-8* | Dolomite | 2.6 | −13.5 | 0.1 | −18.7 | 21.3 | | 6514 | tr. | – |
| MM-10* | Argillite | | | 0.1 | −20.6 | | | | | |
| Cherty Dolomite Member | | | | | | | | | | |
| MM-11* | Dolomite | 5.6 | −11.0 | | | | | 3472 | 37 | 93.9 |
| MM-12* | Dolomite | 8.2 | −8.5 | 0.1 | −15.9 | 24.1 | | 2669 | 43 | 62.2 |

Table 1 (*Continued*)

| Sample # | Analyzed mineral/rock | $\delta^{13}C_{carb}$ (‰, V-PDB) | $\delta^{18}O_{carb}$ (‰, V-PDB) | TOC (mg C/g sample) | $\delta^{13}C_{org}$ | $\Delta^{13}C_{carb-org}$ | Fe (%) | Mn (ppm) | Sr (ppm) | Mn/Sr | $^{87}Sr/^{86}Sr$ |
|---|---|---|---|---|---|---|---|---|---|---|---|
| MM-13* | Dolomite | 5.3 | −12.5 | | | | | 1245 | tr. | – | |
| MM-14* | Dolomite | 8.0 | −8.8 | | | | | 1397 | 39 | 36.1 | |
| MM-15* | Dolomite | 8.3 | −6.4 | | | | | 991 | 34 | 29.4 | |
| Grey-green Argillite Member | | | | | | | | | | | |
| MM-19* | Argillite | | | 0.14 | −23.6 | | | | | | |
| MM-20* | Dolomite | 4.6 | −13.3 | | | | | 1284 | 25 | 51.8 | |
| MM-21* | Dolomite | 4.5 | −14.5 | 0.1 | −13.5 | 18.0 | | 1842 | 76 | 24.4 | |
| MM-22* | Dolomite | 2.4 | −6.9 | | | | | 1656 | 6 | 265.8 | |
| MM-23* | Argillite | | | 0.1 | −22.0 | | | | | | |
| MM-24* | Dolomite | 3.7 | −13.4 | 0.1 | −15.4 | 19.1 | | 527 | 11 | 48.9 | |
| MM-25* | Dolomite | 3.6 | −12.5 | | | | | 7406 | 49 | 149.7 | |
| MM-26* | Dolomite | 5.7 | −12.0 | 0.1 | −17.8 | 23.5 | | 1448 | 73 | 19.8 | |
| MM-27* | Dolomite | 5.4 | −12.5 | | | | | 2316 | 46 | 50.7 | |
| Middle Quartzite Member | | | | | | | | | | | |
| KO-1-2(2)$ | Dolomite | 5.3 | −16.8 | | | | 0.56 | 2742.2 | 169 | 16.2 | |
| Big Cusp Algal Dolomite Member | | | | | | | | | | | |
| KO-1-3$ | Dolomite | 4.3 | −12.8 | | | | 1.41 | 3808 | 80 | 47.6 | |
| KO-1-4$ | Dolomite | 1.9 | −15.5 | | | | 1.90 | 5089 | 62 | 82.7 | |
| KO-1-5$ | Dolomite | 2.4 | −16.2 | | | | 1.91 | 5641 | 99 | 57.0 | |
| KO-1-6$ | Dolomite | 7.2 | −11.2 | | | | 0.35 | 1824 | 116 | 15.7 | |
| KO-1-7$ | Dolomite | 5.8 | −13.8 | | | | 1.01 | 3544 | 92 | 38.5 | |
| KO-1-8$ | Dolomite | 6.5 | −13.9 | | | | 0.52 | 769 | 142 | 5.4 | |
| KO-1-9$ | Dolomite | 8.3 | −14.6 | | | | 0.27 | 422 | 265 | 1.6 | |
| MM-28* | Dolomite | 5.8 | −10.2 | | | | | 1173 | 352 | 3.3 | |
| MM-29* | Dolomite | 4.0 | −14.2 | 0.1 | −21.6 | 25.7 | | 1992 | 90 | 22.3 | |
| MM-30* | Dolomite | 6.4 | −12.4 | 0.1 | −19.4 | 25.8 | | 1258 | 126 | 10.0 | |
| MM-31* | Dolomite | 6.5 | −11.1 | | | | | 1897 | 42 | 45.6 | |
| MM-32* | Dolomite | 7.1 | −9.8 | | | | | 1388 | 97 | 14.3 | |
| MM-33* | Dolomite | 6.4 | −12.4 | | | | | 1301 | 42 | 30.6 | |
| MM-35* | Dolomite | 6.4 | −11.8 | | | | | 1903 | 75 | 25.2 | |
| MM-36* | Dolomite | 3.3 | −12.0 | | | | | 1970 | 46 | 43.0 | |
| MM-37* | Dolomite | 6.8 | −10.2 | | | | | 4190 | 36 | 116.9 | |
| MM-38* | Dolomite | 7.1 | −9.1 | 0.1 | −11.1 | 18.2 | | 2021 | 95 | 21.2 | |
| Valley Member | | | | | | | | | | | |
| MM-39* | Dolomite | 6.6 | −10.8 | | | | | 1146 | 79 | 14.6 | |
| MM-40* | Dolomite | 7.9 | −11.3 | | | | | 276 | 244 | 1.1 | |
| MM-41* | Dolomite | 9.5 | −10.9 | | | | | 328 | 225 | 1.5 | |
| Color-banded Dolomite Member | | | | | | | | | | | |
| KO-1-10$ | Dolomite | 6.5 | −14.1 | | | | 0.91 | 1048 | 322 | 3.3 | |
| KO-1-11$ | Dolomite | 7.2 | −12.3 | | | | 0.29 | 794 | 320 | 2.5 | |

| | | | | | | | | | | | |
|---|---|---|---|---|---|---|---|---|---|---|---|
| KO-1-12$ | Dolomite | 6.6 | −11.6 | | | | 1.19 | 2545 | 360 | 7.1 | |
| KO-1-13$ | Dolomite | 6.1 | −13.1 | | | | 0.35 | 1692 | 152 | 11.1 | |
| KO-1-14$ | Dolomite | 7.2 | −12.6 | | | | 0.57 | 1594 | 874 | 1.8 | |
| KO-1-15$ | Dolomite | 7.5 | −13.0 | | | | 0.51 | 2087 | 283 | 7.4 | |
| KO-1-16$ | Dolomite | 7.4 | −12.9 | | | | 0.42 | 1865 | 524 | 3.6 | |
| KO-1-17$ | Dolomite | 7.4 | −12.6 | | | | 0.21 | 1033 | 233 | 4.4 | |
| KO-1-17′$ | Dolomite | 7.4 | −11.8 | | | | 0.22 | 2041 | 150 | 13.6 | |
| KO-1-17a$ | Dolomite | 6.8 | −13.0 | | | | 0.20 | 528 | 301 | 1.8 | |
| MM-42* | Dolomite | 9.4 | −12.4 | 0.1 | −12.3 | 21.7 | | 213 | 141 | 1.5 | |
| MM-43* | Dolomite | 8.9 | −12.5 | 0.1 | −16.1 | 25.0 | | 426 | 73 | 5.9 | |
| MM-44* | Dolomite | 6.6 | −6.6 | | | | | 940 | 73 | 12.9 | |
| MM-45* | Dolomite | 7.0 | −12.0 | | | | | 279 | 130 | 2.1 | |
| MM-46* | Dolomite | 6.8 | −10.8 | | | | | 203 | 112 | 1.8 | |
| MM-47* | Dolomite | 7.6 | −9.6 | | | | | 932 | 252 | 3.7 | |
| MM-48* | Dolomite | 8.0 | −8.5 | | | | | 833 | 537 | 1.6 | |
| MM-49* | Dolomite | 8.0 | −11.1 | 0.04 | −16.1 | 24.1 | | 1009 | 209 | 4.8 | |
| MM-50* | Dolomite | 6.2 | −13.3 | | | | | 542 | 127 | 4.3 | |
| MM-51* | Dolomite | 7.5 | −10.5 | | | | | 497 | 262 | 1.9 | |
| MM-52* | Dolomite | 7.3 | −12.6 | | | | | 1006 | 368 | 2.7 | |
| MM-53* | Dolomite | 7.4 | −7.4 | | | | | 1123 | 271 | 4.1 | |
| MM-54* | Dolomite | 7.1 | −12.2 | | | | | 438 | 279 | 1.6 | |
| MM-56* | Dolomite | 7.1 | −12.9 | | | | | 441 | 331 | 1.3 | |
| MM-57* | Dolomite | 7.1 | −12.3 | | | | | 372 | 257 | 1.5 | |
| MM-58* | Dolomite | 7.1 | −12.3 | 0.1 | −12.3 | 19.4 | | 477 | 201 | 2.4 | |
| MM-59* | Dolomite | 7.6 | −7.9 | | | | | 697 | 183 | 3.8 | |
| MM-60* | Dolomite | 7.3 | −9.1 | | | | | 656 | 137 | 4.8 | |
| Upper Quartzite Member | | | | | | | | | | | |
| KO-1-17b$ | Dolomite | 6.9 | −13.0 | | | | | | | | |
| MM-62* | Dolomite | 6.0 | −12.0 | | | | | 1006 | 276 | 3.6 | |
| Rugged Hills Member | | | | | | | | | | | |
| KO-1-18$ | Dolomite | 6.7 | −12.5 | | | | | | | | |
| KO-1-19$ | Dolomite | 6.6 | −11.8 | | | | 0.21 | 318 | 392 | 0.8 | 0.7050584 |
| KO-1-20$ | Dolomite | 6.2 | −12.9 | | | | 0.17 | 419 | 229 | 1.8 | |
| KO-1-21$ | Dolomite | 6.1 | −11.8 | | | | 0.14 | 331 | 436 | 0.8 | 0.7049118 |
| KO-1-21′$ | Dolomite | 5.7 | −13.7 | | | | 0.28 | 537 | 177 | 3.0 | |
| MM-63* | Dolomite | 7.1 | −10.6 | 0.1 | −15.2 | 22.3 | | 271 | 130 | 2.1 | |
| MM-64* | Dolomite | 6.8 | −9.8 | | | | | 286 | 184 | 1.6 | |
| MM-65* | Dolomite | 6.3 | −10.2 | | | | | 114 | 182 | 0.6 | |
| MM-66* | Dolomite | 6.5 | −9.1 | | | | | 44 | 199 | 0.2 | |
| MM-68* | Dolomite | 6.5 | −9.7 | | | | | 335 | 199 | 1.7 | |
| MM-69* | Dolomite | 5.8 | −12.3 | 0.18 | −25.6 | 31.3 | | 626 | 126 | 5.0 | |
| MM-70* | Dolomite | 6.4 | −9.0 | | | | | 613 | 135 | 4.6 | |
| MM-71* | Dolomite | 5.9 | −8.9 | | | | | 264 | 41 | 6.4 | |
| MM-72* | Dolomite | 7.0 | −8.7 | | | | | 289 | 118 | 2.5 | |
| MM-73* | Dolomite | 6.1 | −11.6 | | | | | 214 | 140 | 1.5 | |

Table 1 (*Continued*)

| Sample # | Analyzed mineral/rock | $\delta^{13}C_{carb}$ (‰, V-PDB) | $\delta^{18}O_{carb}$ (‰, V-PDB) | TOC (mg C/g sample) | $\delta^{13}C_{org}$ | $\Delta^{13}C_{carb-org}$ | Fe (%) | Mn (ppm) | Sr (ppm) | Mn/Sr | $^{87}Sr/^{86}Sr$ |
|---|---|---|---|---|---|---|---|---|---|---|---|
| MM-74* | Dolomite | 6.1 | −12.0 | 0.1 | −22.4 | 28.5 | | 389 | 113 | 3.4 | |
| MM-75* | Dolomite | 3.4 | −11.4 | | | | | 1216 | 75 | 16.2 | |
| MM-76* | Dolomite | 6.4 | −10.7 | | | | | 312 | 252 | 1.2 | |
| MM-77* | Dolomite | 6.7 | −11.2 | | | | | 296 | 172 | 1.7 | |
| MM-78* | Dolomite | 6.6 | −10.7 | | | | | 335 | 149 | 2.2 | |
| MM-79* | Dolomite | 6.4 | −12.5 | | | | | 321 | 271 | 1.2 | |
| MM-80* | Dolomite | 6.6 | −12.9 | | | | | 24 | 128 | 0.2 | |
| MM-81* | Dolomite | 6.0 | −12.0 | | | | | 312 | 41 | 7.6 | |
| MM-82* | Dolomite | 5.9 | −9.6 | | | | | 617 | 89 | 6.9 | |
| MM-83* | Dolomite | 5.8 | −11.5 | | | | | 582 | 114 | 5.1 | |
| MM-85* | Dolomite | 5.8 | −13.1 | 0.1 | −17.0 | 22.8 | | 2598 | 71 | 36.6 | |
| MM-86* | Dolomite | 4.3 | −11.7 | | | | | 2160 | 27 | 81.2 | |
| MM-88* | Dolomite | 5.9 | −11.4 | | | | | 1205 | 156 | 7.7 | |
| MM-89* | Dolomite | 5.7 | −11.0 | 0.1 | −13.7 | 19.4 | | 2166 | 66 | 32.8 | |
| MM-90* | Dolomite | 5.4 | −10.9 | | | | | 2962 | 44 | 67.6 | |
| MM-91* | Dolomite | 5.0 | −10.5 | | | | | 3145 | 111 | 28.3 | |
| Randville Formation | | | | | | | | | | | |
| Crystal Falls District, MI, collected by USGS | | | | | | | | | | | |
| 24973-USGS$ | Dolomite | 2.1 | −9.3 | | | | 0.56 | 806 | 54 | 14.9 | |
| SE1/4, Sec. 4, T.43N, R.31W, Kiernan Quadrangle, Iron County, MI | | | | | | | | | | | |
| RA-1-1$ | Dolomite | 1.1 | −15.5 | | | | 2.52 | 2020 | 111 | 18.2 | |
| RA-1-2$ | Dolomite | 0.5 | −14.2 | | | | 2.70 | 2520 | 108 | 23.3 | |
| Central part of Sec. 4, T.43N, R.31W, Kiernan Quadrangle, Iron County, MI | | | | | | | | | | | |
| RA-2-1$ | Dolomite | 2.6 | −10.8 | | | | 0.77 | 519 | 78 | 6.7 | |
| RA-2-2$ | Dolomite | 3.1 | −8.2 | | | | 0.47 | 324 | 69 | 4.7 | |
| RA-2-3$ | Dolomite | 3.1 | −8.2 | | | | 0.55 | 405 | 60 | 6.8 | |
| RA-2-4$ | Dolomite | 2.9 | −9.1 | | | | 0.53 | 366 | 71 | 5.2 | |
| S1/2, Sec. 5, T.43N, R.28W, Central Dickinson County, MI. | | | | | | | | | | | |
| RA-3-1$ | Dolomite | 0.2 | −11.1 | | | | 0.34 | 969 | 46 | 21.2 | |
| RA-3-2$ | Dolomite | 0.4 | −12.0 | | | | 0.44 | 542 | 62 | 8.7 | |
| RA-3-3* | Dolomite | 0.8 | −7.1 | | | | | | | | |
| Border of Sec. 3 & 4, T.43N, R.28W, Central Dickinson County, MI. | | | | | | | | | | | |
| RA-4-1$ | Dolomite | 1.4 | −10.0 | | | | 0.76 | 400 | 75 | 5.3 | |
| RA-4-2* | Dolomite | 1.3 | −7.0 | | | | | | | | |
| NE1/4, SE1/4, Sec. 29, T.40N, R.30W, Iron Mountain, Dickinson County, MI | | | | | | | | | | | |
| RA-5-1$ | Dolomite | 1.5 | −7.9 | | | | 0.51 | 173 | 72 | 2.4 | |
| RA-5-2* | Dolomite | 1.4 | −6.9 | | | | | | | | |

| | | | | | | | |
|---|---|---|---|---|---|---|---|
| RA-5-3* | Dolomite | 1.3 | −6.3 | | | | |
| RA-5-6* | Dolomite | 1.3 | −6.4 | | | | |
| RA-5-8$ | Dolomite | 1.2 | −10.1 | 0.50 | 196 | 78 | 2.5 |
| RA-5-9* | Dolomite | 1.4 | −6.3 | | | | |
| RA-5-10* | Dolomite | 1.1 | −5.9 | | | | |
| NE1/4, Sec. 2, T.39N, R.30W, Iron Mountain, Dickinson County, MI | | | | | | | |
| RA-6-1$ | Dolomite | −0.2 | −9.2 | 0.40 | 477 | 92 | 5.2 |
| RA-6-2* | Dolomite | −0.2 | −7.4 | | | | |
| RA-6-3* | Dolomite | −0.3 | −7.5 | | | | |
| S1/2, Sec. 35, T.40N, R.30W, Iron Mountain, Dickinson County, MI | | | | | | | |
| RA-7-2* | Dolomite | 0.6 | −10.0 | | | | |
| RA-7-3* | Dolomite | 1.1 | −8.6 | | | | |
| RA-7-4* | Dolomite | 1.2 | −6.3 | | | | |
| RA-7-5$ | Dolomite | 0.8 | −9.9 | 0.30 | 427 | 45 | 9.5 |
| RA-7-6* | Dolomite | 0.9 | −8.6 | | | | |
| NE1/4, Sec. 2, T.39N, R.30W, Iron Mountain, Dickinson County, MI | | | | | | | |
| RA-8-1$ | Dolomite | 0.9 | −8.0 | 0.49 | 220 | 35 | 6.3 |
| SE1/4, Sec. 12, T.39N, R.29W, Loretto, Dickinson County, MI | | | | | | | |
| LO-1* | Dolomite | 1.4 | −7.7 | | 70 | 42 | 1.7 |
| LO-2* | Dolomite | 0.5 | −7.6 | | 140 | 52 | 2.7 |
| LO-3* | Dolomite | 1.9 | −5.6 | | 149 | 59 | 2.5 |
| LO-4* | Dolomite | −0.4 | −11.5 | | 442 | 92 | 4.8 |
| LO-5* | Dolomite | 1.8 | −5.9 | | 211 | 22 | 9.8 |
| LO-6.Ar* | Dolomite | 1.3 | −7.8 | | 323 | tr. | – |
| LO-6.Aw* | Dolomite | 0.4 | −9.3 | | 98 | 106 | 0.9 |
| LO-6.6B* | Dolomite | 1.5 | −7.3 | | 223 | tr. | – |
| Saunders Formation | | | | | | | |
| Brule River, on the border of Sec. 19 and Sec. 30, T.4N, R.16E, WI (James et al., 1968) | | | | | | | |
| SA-2$ | Dolomite | 1.6 | −12.6 | 0.55 | 328.5 | 56.3 | 5.8 |
| SA-3$ | Dolomite | 1.3 | −12.6 | 0.57 | 404.6 | 61.9 | 6.5 |
| SA-4$ | Dolomite | 1.4 | −13.6 | 0.48 | 536.3 | 68.7 | 7.8 |
| SA-5$ | Dolomite | −0.8 | −16.0 | 0.91 | 667.4 | 81.5 | 8.2 |
| SA-6$ | Dolomite | 0.6 | −13.6 | 0.62 | 396.8 | 91.9 | 4.3 |
| SA-7* | Dolomite | 2.1 | −10.0 | | | | |
| SA-9$ | Dolomite | 1.9 | −11.7 | 0.37 | 300.5 | 57.6 | 5.2 |
| SA-10$ | Dolomite | 2.4 | −11.1 | 0.17 | 160.4 | 48.3 | 3.3 |
| SA-12$ | Dolomite | −1.2 | −15.0 | 2.18 | 676.1 | 119.0 | 5.7 |
| SA-13$ | Dolomite | 0.4 | −16.4 | 0.60 | 340.2 | 51.6 | 6.6 |
| SA-14$ | Dolomite | 1.5 | −13.2 | 0.43 | 196.8 | 61.8 | 3.2 |
| Brule River, on the border of Sec. 25 and Sec. 26, T.41N, R.15E, WI (James et al., 1968) | | | | | | | |
| SA-2-1* | Dolomite | −2.5 | −12.5 | | | | |
| SA-2-3* | Dolomite | −1.4 | −13.9 | | | | |

Table 1 (*Continued*)

| Sample # | Analyzed mineral/rock | $\delta^{13}C_{carb}$ (‰, V-PDB) | $\delta^{18}O_{carb}$ (‰, V-PDB) | TOC (mg C/g sample) | $\delta^{13}C_{org}$ | $\Delta^{13}C_{carb-org}$ | Fe (%) | Mn (ppm) | Sr (ppm) | Mn/Sr | $^{87}Sr/^{86}Sr$ |
|---|---|---|---|---|---|---|---|---|---|---|---|
| Bad River Dolomite | | | | | | | | | | | |
| SE1/4, Sec. 18, T.47N, R.44W, Wakefield NE 7.5 min Quadrangle, MI | | | | | | | | | | | |
| BD-W-96-4* | Dolomite | 1.8 | −7.7 | | | | | | | | |
| MI-BR-1$ | Dolomite | −0.1 | −9.2 | | | | 0.87 | 1968 | 25 | 78.1 | |
| MI-BR-2$ | Dolomite | −0.2 | −8.9 | | | | 0.37 | 888 | 36 | 24.7 | |
| Grand View Quarry, NW1/4, NW1/4, NW1/4, Sec. 22, T.44N, R.5W, Marengo 7.5 min Quadrangle, Bayfield County, WI | | | | | | | | | | | |
| BD-96-1* | Dolomite | 2.4 | −8.3 | | | | | | | | |
| BD-96-2$ | Dolomite | 1.2 | −11.1 | | | | 0.58 | 550 | 32 | 17.1 | |
| BD-96-3$ | Dolomite | 2.0 | −10.5 | | | | 0.49 | 534 | 34 | 15.6 | |
| BD-96-4$ | Dolomite | 1.9 | −9.0 | | | | 0.43 | 437 | 39 | 11.3 | |
| BD-96-5$ | Dolomite | 1.0 | −10.8 | | | | 0.43 | 562 | 34 | 16.4 | |
| BD-96-6$ | Dolomite | 2.1 | −9.3 | | | | 0.47 | 466 | 29 | 16.3 | |
| BD-96-7* | Dolomite | 2.3 | −7.4 | | | | | | | | |
| BD-96-8* | Dolomite | 1.5 | −8.6 | | | | | | | | |
| BD-96-9* | Dolomite | 0.7 | −11.5 | | | | | | | | |
| BD-96-10$ | Dolomite | 1.0 | −9.4 | | | | 0.51 | 400 | 41 | 9.7 | |
| BD-96-12$ | Dolomite | 1.3 | −9.3 | | | | 0.49 | 397 | 32 | 12.6 | |
| E1/2, NW1/4, Sec. 24, T.44N, R.4W, Mineral Lake 7.5 min Quadrangle, Ashland County, WI | | | | | | | | | | | |
| 9653* | Dolomite | 0.5 | −7.1 | | | | | | | | |
| NE1/4, SE1/4, NW1/4, Sec. 14, T.44N, R.3W, Mellen 7.5 min Quadrangle, Ashland County, WI | | | | | | | | | | | |
| BD-PN-1* | Dolomite | −0.5 | −7.7 | | | | | | | | |
| BD-PN-2* | Dolomite | −0.3 | −7.4 | | | | | | | | |
| Paleoproterozoic carbonate, Watersmeet Dome, MI | | | | | | | | | | | |
| NE1/4, Sec. 5, T.45N, R.40W, Watersmeet, MI | | | | | | | | | | | |
| WD-1* | Dolomite | 0.0 | −13.7 | | | | | 338 | 25 | 13.7 | |
| WD-1.2* | Dolomite | −0.2 | −14.1 | | | | | 418 | 21 | 20.1 | |
| Trout Lake Formation, Emily District, Cuyuna Range, MN (Drillcore 18224; University of Minnesota, Duluth; NE1/4, NE1/4, Sec. 32, T.138N, R.26W) | | | | | | | | | | | |
| MN-1-391$ | Dolomite | 0.3 | −6.8 | | | | 0.15 | 385 | 39 | 9.8 | |
| MN-2-395$ | Dolomite | −0.2 | −8.4 | | | | 0.36 | 1561 | 52 | 29.9 | |
| MN-3-408$ | Dolomite | 0.3 | −9.2 | | | | 0.39 | 471 | 51 | 9.2 | |
| MN-4-420$ | Dolomite | 0.3 | −6.5 | | | | 0.17 | 241 | 38 | 6.3 | |
| MN-5-435$ | Dolomite | 0.4 | −8.6 | | | | 0.56 | 661 | 40 | 16.7 | |
| MN-6-451$ | Dolomite | 0.2 | −8.4 | | | | 0.34 | 764 | 44 | 17.6 | |
| MN-7-463$ | Dolomite | 0.4 | −8.4 | | | | 0.46 | 505 | 37 | 13.8 | |
| MN-8-481$ | Dolomite | 0.1 | −8.6 | | | | 0.32 | 410 | 51 | 8.1 | |
| MN-9-510$ | Dolomite | −0.1 | −9.6 | | | | 0.32 | 309 | 55 | 5.6 | |
| MN-10-514$ | Dolomite | 0.3 | −9.4 | | | | 0.90 | 830 | 44 | 18.7 | |

| | | | | | | | |
|---|---|---|---|---|---|---|---|
| Denham Formation | | | | | | | |
| Outcrop in the Birch Creek valley ~1.6 km SE of Denham (NE1/4, SE1/4, Sec. 25, T.45N, R.21W) | | | | | | | |
| BE-96-D-2$ | Dolomite | 1.8 | −14.4 | 2.18 | 904.6 | 93 | 9.8 |
| BE-96-D-4$ | Dolomite | 1.5 | −15.6 | 1.36 | 1071.0 | 110 | 9.8 |
| BE-96-D-5$ | Dolomite | 0.6 | −11.0 | 1.71 | 1139.0 | 30 | 38.1 |
| BE-96-D-7$ | Dolomite | 1.0 | −10.2 | 0.98 | 621.1 | 31 | 19.9 |
| Ryb-1/1$ | Dolomite | 1.0 | −10.1 | 0.81 | 895.8 | 36 | 25.0 |
| Ryb-5b$ | Dolomite | −2.6 | −15.3 | 1.82 | 2393.6 | 101 | 23.7 |
| BM-1 Drillcore, Sec. 16, T.47N, R.19W, Carlton County, MN (Severson et al., 2003) | | | | | | | |
| BM-1-2323 | Dolomite | 1.7 | −11.3 | | | | |
| BM-1-2606 | Dolomite | 1.7 | −10.1 | | | | |
| BM-1-2658 | Dolomite | 2.1 | −13.5 | | | | |
| BM-1-2780 | Dolomite | 1.3 | −8.8 | | | | |
| BM-1-2810 | Dolomite | 1.4 | −12.3 | | | | |
| BM-1-2853 | Dolomite | 2.1 | −12.6 | | | | |
| BM-1-2863 | Dolomite | 1.9 | −12.8 | | | | |
| BM-1-2873 | Dolomite | 2.5 | −12.2 | | | | |
| Glen Township Formation | | | | | | | |
| Drill core A-6, Sec. 20, T.46N, R.25W (Severson et al., 2003) | | | | | | | |
| A-6-2986 | Dolomite | 0.3 | −15.3 | | | | |
| A-6-2988 | Dolomite | −0.1 | −16.2 | | | | |
| A-6-2990 | Dolomite | 0.2 | −16.3 | | | | |
| A-6-2994 | Dolomite | −1.0 | −16.2 | | | | |
| A-6-3001 | Dolomite | −0.4 | −15.9 | | | | |
| A-6-3004 | Dolomite | −1.2 | −15.1 | | | | |
| A-6-3005.5 | Dolomite | −0.1 | −15.5 | | | | |
| A-6-3007 | Dolomite | −0.2 | −14.9 | | | | |
| A-6-3009 | Dolomite | −0.4 | −15.5 | | | | |

Analytical uncertainties are better than 10% for Mn, Fe and Sr, based on repeated analyses of standard materials. C and O isotope values, and major and trace element concentrations for all samples except those marked with an asterisk were measured at the Geological Survey of Finland. Whole rock analyses are marked with a dollar sign. The external precision of isotopic measurements at the Geological Survey of Finland is better than 0.1‰ for both carbon and oxygen based on multiple analysis of the NBS-19 carbonate standard. For samples marked with an asterisk, C and O isotope values of carbonates and TOC content were measured at the University of Maryland; carbon isotope values of organic carbon were measured at the Mountain Mass Spectrometry; trace element contents was measured at VPI & SU. Samples with carbonate content below 50% were not analyzed for major and trace elements.

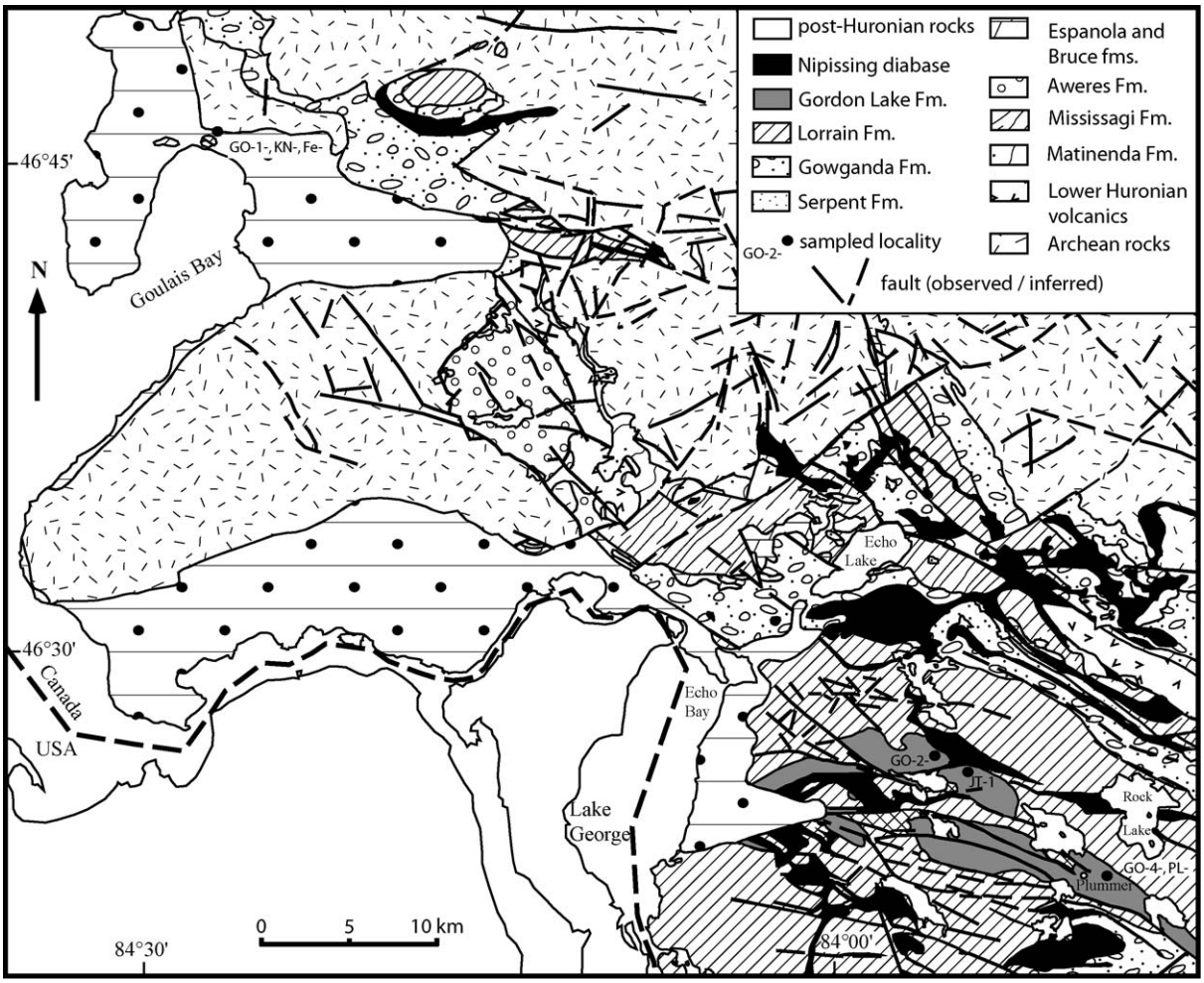


Fig. 3. Geological map of the eastern part of the Huronian basin with sampled localities of the Gordon Lake Formation shown (modified from Giblin et al., 1976).

are abruptly but concordantly overlain by iron-rich siltstones and sandstones. Calcarenites in the upper part of the section contain oölites, subrounded to well-rounded quartz grains, angular to subrounded sand-size clasts of dolomicrite, and pink barite lenses (Bennett et al., 1989).

In Aberdeen Additional and Meredith townships, siliceous green dolomites form thin stratiform nodules, lenses (up to 15–20 cm thick) and at least three recessive layers with thickness up to several decimeters in varicolored coarse-grained arkosic sandstones and mudstones with low-angle cross-bedding, chert nodules, symmetrical wave ripples, and mudcracks in the lower 20 m of the Gordon Lake Formation. Chert likely replaced anhydrite in nodules (cf. Chandler, 1988). In Plummer Township, seven dolomite beds from 5 to 20 cm thick occur in a 8.6 m thick section of varicolored silicified arkosic sandstone with asymmetrical ripple marks.

Dolomites and calcareous siltstone beds in the Killarney Bay area (Frarey, 1985) that are considered correlative with the Gordon Lake Formation experienced amphibolite facies of metamorphism (Card, 1978). They contain varicolored siliciclastic layers with wave ripples that have internal cross-laminations, syneresis cracks, breccias, cross-, flaser, and convoluted bedding, ball and pillow structures, and soft-sediment deformation structures indicating deposition in shallow to deeper water environments with high sedimentation rates and slope instability.

### *4.1.1. Geochemical data*

Forty-five samples of the Gordon Lake Formation dolomites including four samples from the Killarney Bay area were analyzed. These dolomites occur over a short stratigraphic and poorly exposed interval at the base of the formation. Carbon isotope values of the

Table 2
$\delta^{34}$S values of barite samples from the Gordon Lake Formation of Fenwick Township

| Sample # | $\delta^{34}$S, ‰ V-CDT |
|---|---|
| GLFa | 12.2 |
| GLFa | 12.4 |
| GLFa | 12.7 |
| GLF-FE-1 | 12.9 |
| GLF-FE-2 | 12.0 |
| GLF-FE-3 | 12.4 |
| GLF-FT-a | 11.7 |
| GLF-FT-b | 11.7 |
| GLF-FT | 11.8 |
| GO-1-15 | 12.3 |
| BaSO4 | 12.2 |
| Average value | 12.2 |
| Standard deviation | 0.38 |

thin, interbedded Gordon Lake Formation dolomites are highly variable ranging from −1 to +8.2‰ versus V-PDB (Table 1); these do not reveal any apparent stratigraphic trend. Oxygen isotope values are also highly variable ranging from −19.6 to −8.6‰ versus V-PDB. Fe and Mn concentrations are high ranging from 0.33 to 1.04% and 320 to 11,562 ppm, respectively. Strontium concentrations are low ranging from trace amounts to 206 ppm and Mn/Sr ratios are all above 3. The four samples from the Killarney Bay area have strongly negative $\delta^{13}$C compositions and are geochemically distinct from dolomites of the Gordon Lake Formation (Table 1). While the difference might partially reflect a higher metamorphic grade in this area, we suggest that their protolith is not correlative with the Gordon Lake Formation. Rejecting samples with low $\delta^{18}$O values and Sr contents and with high contents of both Fe and Mn, the range of carbon isotope values narrowed to +5.0 to +8.2‰, which we interpret to reflect primary composition of carbonates from the Gordon Lake Formation. Eleven analyses of barite samples from the Gordon Lake Formation, Fenwick Township show narrow range of $\delta^{34}$S values with the average of 12.2 ± 0.4‰ versus V-CDT (Table 2).

### 4.2. Kona Dolomite, Marquette Range Supergroup, Marquette, MI, USA

The Kona Dolomite of the Marquette Range lies above the mature Mesnard Quartzite and the underlying glacially-influenced Enchantment Lake Formation and is overlain by the Wewe Slate (Fig. 2). The age of the Enchantment Lake Formation is bracketed by the age of the youngest detrital zircon of 2288 ± 15 Ma and the age of the oldest hydrothermal xenotime of 2133 ± 11 Ma (Vallini et al., in press). The Kona Dolomite was metamorphosed to chlorite-biotite grade during the Penokean Orogeny and outcrops in the eastern part of the Marquette Trough, a broad EW-trending belt of Paleoproterozoic rocks (Fig. 4). It reaches 870 m in thickness and is subdivided into 11 informal members (Taylor, 1972). The lower contact is gradational over the 3 m thick section. The lower part is more argillitic and arenitic while the upper part is predominantly dolomitic and consists of upward-shallowing cycles of stromatolitic dolomites capped by pink-purple mudstones and mature sandstones with mudcracks and pseudomorphs and molds of sulfates and halite. The Kona Dolomite in the eastern part of the Marquette Trough consists of white to dark-brown cherty dolomicrite, intradolomicrite, and dolosparite interstratified with layers of slate, graywacke, and sandstone but changes to sandstone, ferruginous mudstone, and chert breccia to the west indicating proximity to the shoreline (Taylor, 1972; Puffett, 1974; Gair, 1975). Micrites of the Kona Dolomite were recrystallized into pseudodolospar during diagenesis and metamorphism (Wohlabaugh, 1980). Pseudomorphs after gypsum and anhydrite (Fig. 5A–C), teepee structures, oöilites, peloids, pisolites, halite hoppers, red beds, copper stratiform deposits, mudcracks, crossbedding, domal and stratiform stromatolites, rosette conglomerates, and imbricated oncolites of the Kona Dolomite likely reflect shallow-marine arid lagoonal settings behind the barrier bar for the lower part and open tidal-flat settings for the upper part (Taylor, 1972; Clark, 1974; Wohlabaugh, 1980). Large columnar stromatolites of *Collenia* sp. (Fig. 5D; Twenhofel, 1919) of the open-marine 35 m thick Big Cusp Algal Dolomite Member form stacked hemispheroids with east-west elongation and eastward oversteepening (Taylor, 1972; Wohlabaugh, 1980; Wohlabaugh and Mancuso, 1990).

Previous sulfur isotope analyses of sulfate-bearing chert pseudomorphs have $\delta^{34}$S values ranging from +11.4 to +16.0‰ with the average $\delta^{34}$S value +13.8‰ (Hemzacek et al., 1982; Hemzacek, 1987; Perry et al., 1984; Feng, 1986). Wohlabaugh (1980) described silicified evaporite beds and collapse breccias in the Big Cusp Algal Dolomite Member. Oöilites are present in the upper part of the formation (Taylor, 1972). Copper stratiform mineralization confined to the lower quartzite member (Fig. 6) developed during diagenesis by replacement of pyrite framboids and euhedral crystals (Clark, 1974). The conformably overlying Wewe Slate has at the contact organic-rich pyriferous shales suggesting basin deepening and contains several horizons of mafic ash beds likely related to reactivation in the Chocolay Basin (Gair and Thaden, 1968). Analyzed samples came from three areas: (1) Mount Mesnard, (2) Lindberg pit, and

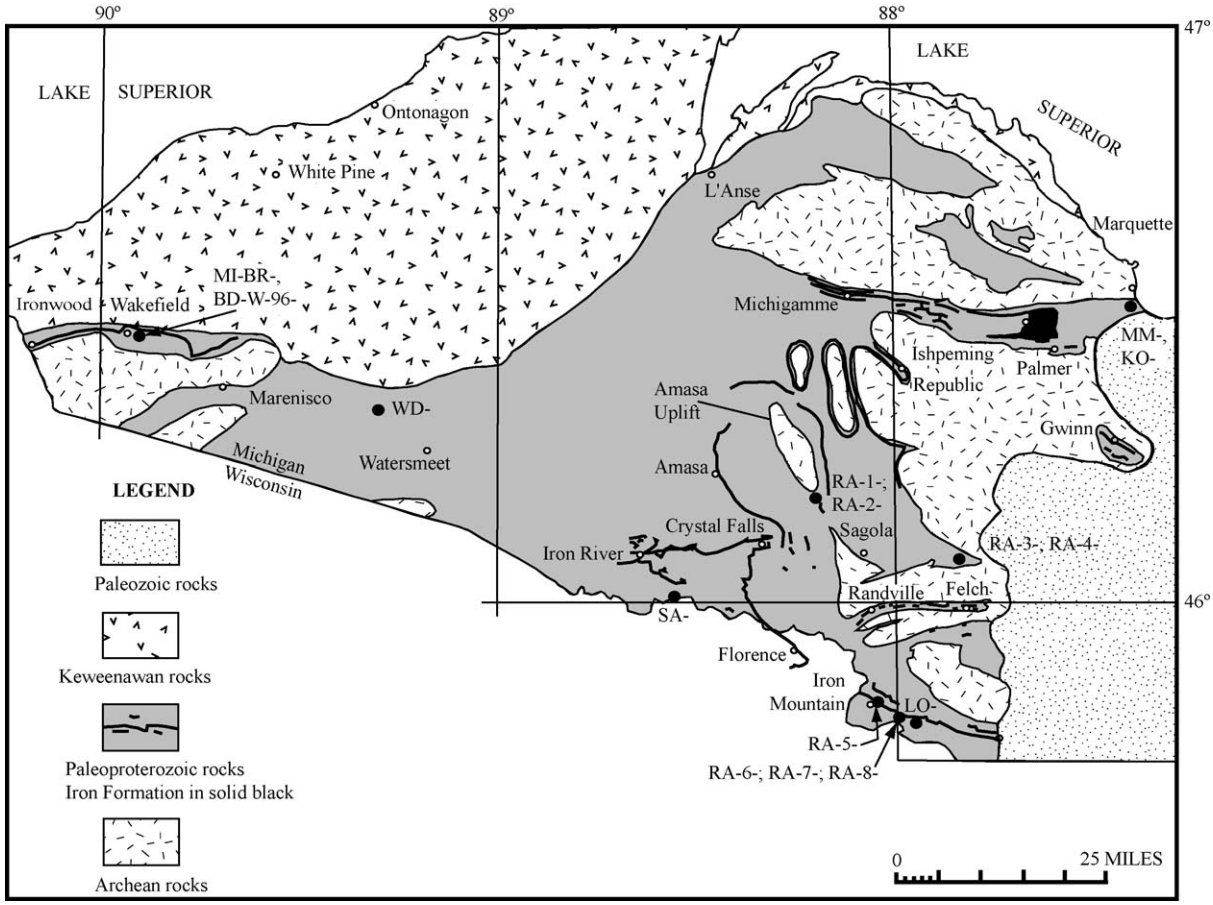


Fig. 4. Schematic geological map of the northern MI and WI with sampled localities of the Chocolay Group shown (modified from Wier, 1967). Note that only the eastern part of the Gogebic Range shown.

(3) State Highway 28 roadcut outside of Marquette, MI. Samples from Mount Mesnard were tied to the informal members of Taylor (1972) (see Fig. 6).

#### 4.2.1. Geochemical data

One hundred and seven dolomite and five argillite samples were analyzed in this study. Carbonates have carbon isotope values ranging from +1.9 to +9.5‰ versus V-PDB and oxygen isotope values ranging from −17.1 to −6.4‰ versus V-PDB. Both dolomites and argillites have low total organic carbon (TOC) contents (0.04–0.18 mg C/g sample) with variable organic carbon isotope compositions (−25.6 to −11.1‰). Fractionation between organic and carbonate carbon is quite variable, ranging from 18.0 to 31.3‰ with smaller values likely reflecting equilibration between kerogen and carbonate during metamorphism. Fe and Mn concentrations are variable but generally high ranging from 0.14 to 1.68% and 24 to 7799 ppm, respectively. Strontium concentrations and Mn/Sr ratios are also highly variable from trace amounts to 874 ppm and 0.2–266, respectively. Samples with low oxygen isotope values and Sr concentrations as well as with high Fe and Mn concentrations are interpreted as more altered. Excluding these altered samples, which are generally associated with siliciclastic-rich intervals, results in a smaller range in carbon isotope values for the least altered samples (+5.0 to +9.5‰). Notably, carbon isotope values decrease towards the top of the stratigraphic section (Fig. 6). Sr isotope values were measured for two samples with small Mn concentrations and Mn/Sr ratios of 0.8. The Sr isotope values are similar (0.7051 and 0.7049) and likely reflect Sr isotope composition of seawater at that time.

### 4.3. Randville Dolomite, MI and Saunders Formation, WI, USA

The metamorphic grade of the Randville Dolomite and the correlative Saunders Formation of the Iron River-Crystal Falls district in Michigan and Wiscon-

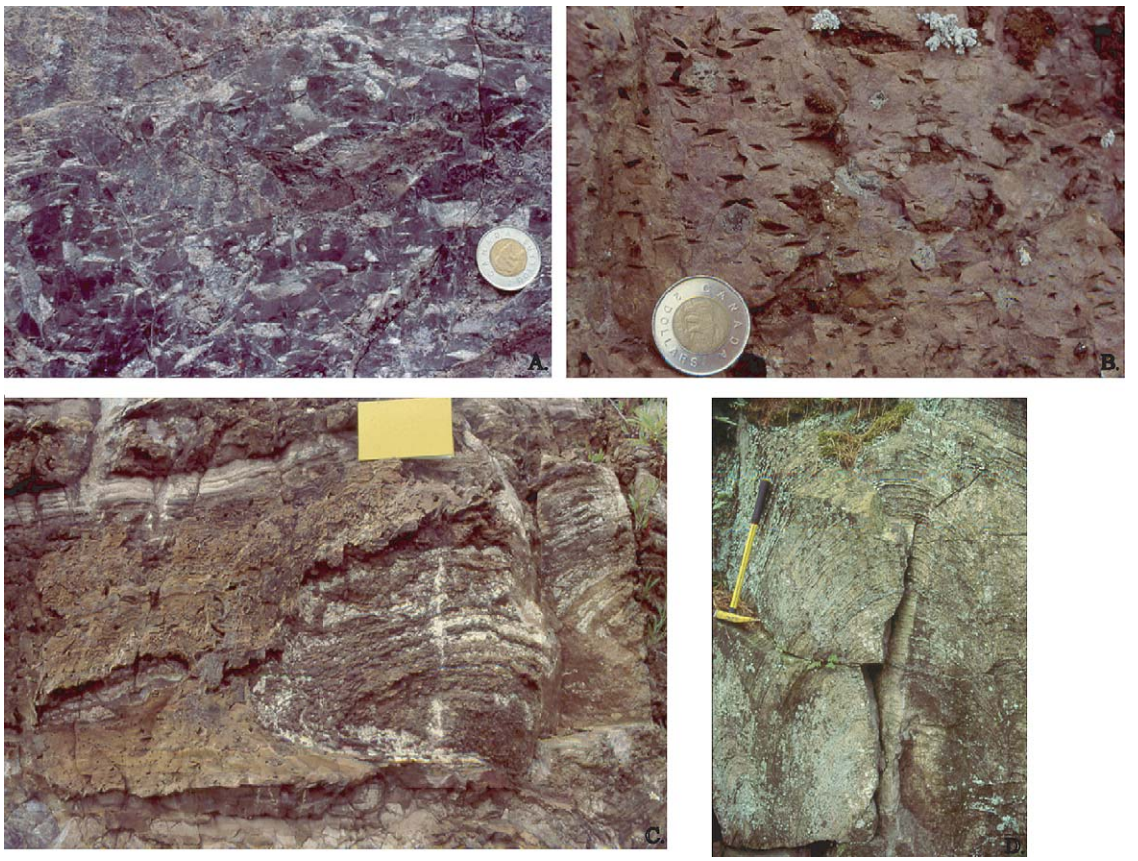


Fig. 5. (A) Chert pseudomorphs after gypsum, Lindberg Pit, MI; (B) molds of gypsum in red-colored siltstone, HW 480 across from Lindberg Pit, MI; (C) stromatolite dome surrounded by silicified layers with pseudomorphs and molds after gypsum, HW 480, MI; (D) *Collenia* sp. (Twenhofel, 1919), type locality near HW 28, Marquette, MI. Coin is 2 cm in diameter, notebook is 16 cm long, and hammer is 70 cm long.

sin (Fig. 4) ranges from greenschist to amphibolite facies (James, 1955; Bayley et al., 1966; James et al., 1968) and they consist of dolomites with variable amounts of siliciclastics (Larue, 1979). The Randville Dolomite overlies the glacially influenced Fern Creek Formation and mature quartzites of the Sturgeon River Quartzite (Pettijohn, 1943). These units are constrained in age between $2302 \pm 4$ Ma, the age of the youngest detrital zircon, and $2115 \pm 5$ Ma, the age of the oldest hydrothermal xenotime (Vallini et al., in press; Fig. 2). Richardson (1949) described columnar, domal, stratiform, and biscuit-shaped stromatolites of the Randville Dolomite (Fig. 7A). The Saunders Dolomite can only be inferred to be the Paleoproterozoic in age without relying on lithostratigraphic correlation with the Kona and Randville dolomites.

Samples of the Randville Dolomite were collected at the Amasa Uplift, from the Calumet Trough, and the southern margin of the Sagola Basin in central Dickinson County. The Randville Dolomite is up to 600 m thick in the southwestern part of the Amasa Uplift, sits directly on the Archean basement, and consists of white and light-grey to buff and pink (due to hematite) massive to thin-bedded, fine-grained dolomite with chert nodules, stromatolites, oölites, and grapestones; sandy dolomite and dolomitic sandstone; silicified breccia; conglomerate and argillite (Clements and Smyth, 1899; Greenman, 1951; Gair and Wier, 1956). Oölites are between 1 and 3 mm in diameter and have radial and concentric cortical layers (Greenman, 1951) that indicate replacement of calcite precursor (cf. Tucker, 1984). Intraformational breccia and conglomerate, domal stromatolites, wave ripple marks, sandy beds, mudcracks, and cross-bedding indicate peritidal setting. Locally, argillite is present above the Randville Dolomite in the Amasa Uplift area (Bayley, 1959).

The Saunders Formation was defined by Allen (1910) in Wisconsin and consists of cherty dolomite, massive white and pink finely crystalline dolomite with stromatolites, sandy dolomite, and impure calcareous shales. Samples were collected from two areas to the south of the Brule River.

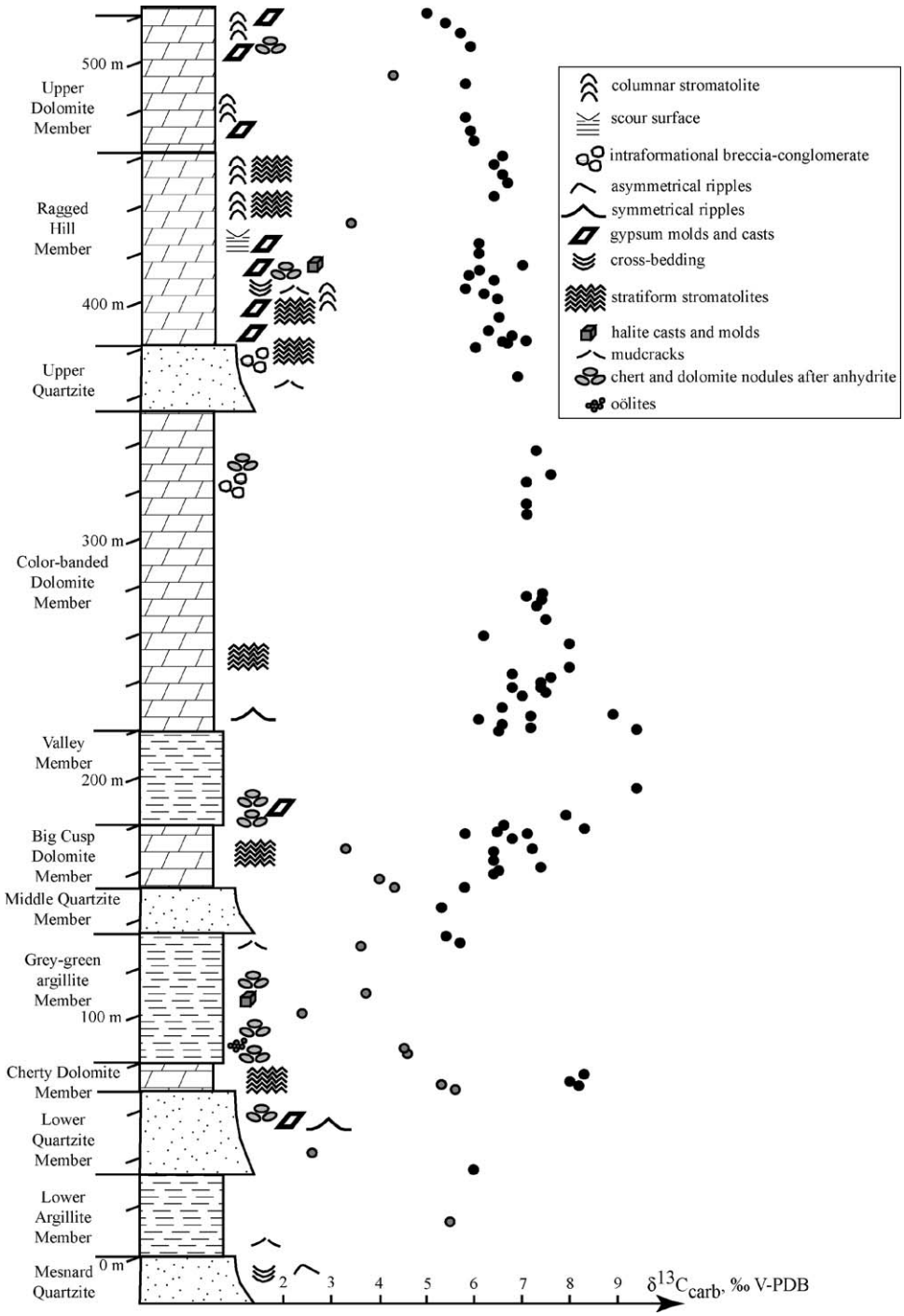


Fig. 6. Stratigraphic column of the Kona Dolomite in the Mount Mesnard area with $\delta^{13}C$ variations shown. Informal members of the Kona Dolomite are from Taylor (1972). Circles show $\delta^{13}C$ data, grey fill indicates highly altered samples based on trace element concentrations, oxygen and carbon isotope values.

Fig. 7. (A) Inclined stromatolites above finely laminated dolomite of the Randville Dolomite, Lake Antoine, Iron Mountain, MI, hammer for scale; (B) small domal stromatolites of the Bad River Dolomite; note grey chert developed along lamina and forming layers above stromatolites; east of Wakefield, MI.

#### 4.3.1. Geochemical data

Thirty-five dolomites of the Randville Dolomite and 13 dolomites of the Saunders Formation were analyzed for this study. Carbon isotope values of the Randville dolomites vary from −0.4 to +3.1‰ and oxygen isotope values range from −15.5 to −5.6‰ (Table 1). Dolomites from the Kiernan Quadrangle have the highest $\delta^{13}C$ values. Iron and Mn concentrations are highly variable from 0.3 to 2.7% and 70 to 2520 ppm, respectively. Strontium concentrations are low ranging from trace amounts to 111 ppm and Mn/Sr ratios are generally high ranging from 0.9 to 23.3.

Carbon isotope values of the Saunders dolomites range from −2.5 to +2.4‰ versus V-PDB and oxygen isotope values vary from −16.4 to −11.1‰ versus V-PDB with the exception of one sample with $\delta^{18}O$ value of −7.2‰. Iron and Mn concentrations are variable from 0.17 to 0.91% and 160 to 667 ppm, respectively. Strontium concentrations are low ranging from 48 to 119 ppm and Mn/Sr ratios are generally high from 3.2 to 8.2. Excluding samples with low oxygen isotope values and Sr concentrations and with high Fe and Mn concentrations and Mn/Sr ratios, primary carbon isotope composition of the Saunders dolomites is between −0.4 and +2.4‰.

### 4.4. Bad River Dolomite, Wisconsin

The Bad River Dolomite sits above the tidally-influenced mature Sunday Quartzite at the eastern end of the Gogebic Range and directly above Archean basement at the western end; both units are absent in the central part of the range (Fig. 1; Schmidt, 1980; LaBerge et al., 1992). The contact between the Sunday Quartzite and Bad River Dolomite is transitional. The age of the Sunday Quartzite and conformably overlying Bad River Dolomite is constrained between the 2637 ± 7 Ma age of the youngest detrital zircon and the 2207 ± 5 Ma age of the oldest hydrothermal xenotime that corresponds to the age of the Nipissing and Senneterre dykes and sills of the Superior Craton (Vallini et al., in press). The Bad River Dolomite in the Grand View area of the western Gogebic Range form an upward-shallowing sequence grading from massive dolomite at the base to cherty, siliciclastics-rich, bedded upper part (Komatar, 1972). The top of the Bad River Dolomite is often brecciated and silicified below the unconformably overlying Menominee Group (Leith, 1925). The Bad River Dolomite consists of grey to buff dolomite with white and black chert layers and nodules, and stromatolites (Fig. 7B); sandstone; and mudchip conglomerate. Wavy and cross-bedding is rarely observed in this unit. The degree of metamorphism ranges from greenschist to amphibolite facies and generally increases to the east. A correlative dolomite (Cannon, 1980; Sims et al., 1984; Sims, 1990) was sampled near Watersmeet, MI (Fig. 4).

#### 4.4.1. Geochemical data

Nineteen dolomites of the Bad River Dolomite were analyzed in this study (Table 1). Carbon isotope values range from −0.5 to +2.4‰ and oxygen isotope values from −11.1 to −7.1‰. Iron and manganese concentrations have small range from 0.37 to 0.87% and 338 to 1968 ppm, respectively. Strontium concentrations are low (21–41 ppm) and, therefore, Mn/Sr ratios are high (9.7–78.1).

### 4.5. Trout Lake, Glen Township, and Denham formations of the Mille Lacs Group, Minnesota

The Mille Lacs Group underlies the ∼1878–1777 Ma Animikie Group with either tectonic or unconformable contact and confined to the Penokean Orogen of east-central Minnesota (Morey and Southwick, 1995;

Ojakangas et al., 2001; Addison et al., 2005; Heaman and Easton, 2005). The Mille Lacs Group occurs in four separate structural terranes making correlation of sedimentary successions between these terranes problematic (Morey, 1996). The group is intruded by the 2009 ± 7 Ma Mille Lacs Granite in the Moose Lake-Glen Township structural terrane (Holm et al., 2005; see Boerboom et al., 1999 for map relationships). Both the sediments and the intrusion may be related to rifting on the southern margin of the Superior Craton dated by the 2076 +5/−4 Ma Kenora-Kabetogama (=Fort Frances) dyke swarm of Northern Minnesota and Ontario (Buchan et al., 1996) and the 2067 ± 1 Ma maf dykes in southwestern Minnesota (Schmitz et al., 2006). The sampled carbonates of the Trout Lake, Glen Township, and Denham formations occur in different terranes, but are considered to be within the upper part of the Mille Lacs Group.

The Trout Lake Formation was correlated with the Bad River Dolomite and other Lake Superior Paleoproterozoic carbonates (Marsden, 1972; Morey, 1972). The Trout Lake Formation is underlain by slates and quartzites of the Mille Lacs Group that unconformably sits on the Archean basement. The carbonate, which contains stratiform stromatolites and is interlayered with quartz sandstone and siltstone, extends for at least 24 km along strike and is at least 27 m thick.

The Denham Formation outcrops near Denham in northwestern Pine County. The unit consists of a 2–3 km thick heterogeneous sequence of quartz arenite and siltstone with up to 10 m of cross-stratified fluvial conglomeratic sandstone at the base, iron formation, up to 330 m of intermediate to mafic volcanic rocks with pillows and amygdaloidal basalt flows, schist, and thick dolomite at the top (Morey, 1978; Boerboom and Jirsa, 2001). The formation sits unconformably on the 2556 ± 10 Ma McGrath Gneiss with a paleosol at the base (Holm, 1986; Boerboom and Jirsa, 2001; Holm et al., 2005) and underlies the Thomson Formation, which is less strongly deformed. The Denham Formation is a Paleoproterozoic rift-passive margin succession (Boerboom and Jirsa, 2001) that was metamorphosed to amphibolite grade (Holm, 1986). The upper part consists of >170 m of dolomite transgressively overlain by a thin sequence of graphitic argillite and greywacke (Boerboom and Jirsa, 2001). The $T_{DM}$ Sm–Nd ages for this unit range from 2.07 to 3.12 Ga (Hemming et al., 1995). Samples were collected from outcrops in Birch Creek approximately 1.6 km southeast of Denham. In addition, carbonates from the lower part of the drill core BM-1 were also sampled. In this drill core, over 530 m of stromatolitic and massive dolomite with thin argillite beds lies beneath a succession of organic-rich argillite with reworked tuffs, arkosic sandstone, and mafic volcanics (Severson et al., 2003).

The Glen Township Formation overlies and passes laterally into the Dam Lake Quartzite, similar to quartz sandstones of the Denham Formation. Conglomerates and quartz sandstones occur in the lower part of the section and grade upwards into thin-bedded fine-grained metasediments with thin dolomite beds, locally developed silicate–carbonate-oxide facies iron formation, carbonaceous shale with sulfides, and basalts (Morey, 1978, 1996; Severson et al., 2003). Mafic volcanics of the Glen Township Formation have tholeiitic to calc-alkaline affinities, carry geochemical signatures indicative of intraplate or continental tectonic settings (Eldougdoug, 1984; Southwick and Morey, 1991), and yielded a Sm–Nd isochron age of 2197 ± 39 Ma (Beck, 1988) that provides a possible maximum age for the Mille Lacs Group. The Glen Township Formation experienced upper greenschist to lower amphibolite facies metamorphism (Eldougdoug, 1984).

#### 4.5.1. Geochemical data

For this study, dolomite samples of the Trout Lake ($n = 10$), Denham ($n = 14$), and Glen Township ($n = 9$) formations were analyzed (Table 1). Dolomites of the Trout Lake Formation have carbon isotope values ranging from −0.2 to +0.4‰ and oxygen isotope values from −9.6 to −6.5‰. Iron and manganese concentrations range from 0.15 to 0.90% and 241 to 1560 ppm, respectively. Strontium concentrations are low from 37 to 55 ppm and Mn/Sr ratios are, therefore, high from 5.6 to 29.9. Dolomites of the Denham Formation have very similar carbon isotope values, ranging from −2.6 to +2.5‰, and oxygen isotope values from −15.6 to −8.8‰. Iron and manganese concentrations range from 0.81 to 2.18% and 621 to 2394 ppm, respectively. Strontium concentrations are low ranging from 30 to 110 ppm and Mn/Sr ratios are high from 9.8 to 38.1. Rejecting one sample with low carbon and oxygen isotope values and high Fe and Mn concentrations and Mn/Sr ratio, primary carbon isotope composition of Denham dolomites is likely between +0.6 and +2.5‰. Dolomites of the Glen Township Formation have carbon isotope values ranging from −1.2 to +0.3‰ and very low oxygen isotope values (−16.3 to −14.9‰) overall.

## 5. Discussion

### 5.1. Diagenesis and metamorphism

Although some of the studied successions experienced amphibolite facies metamorphism resulting in

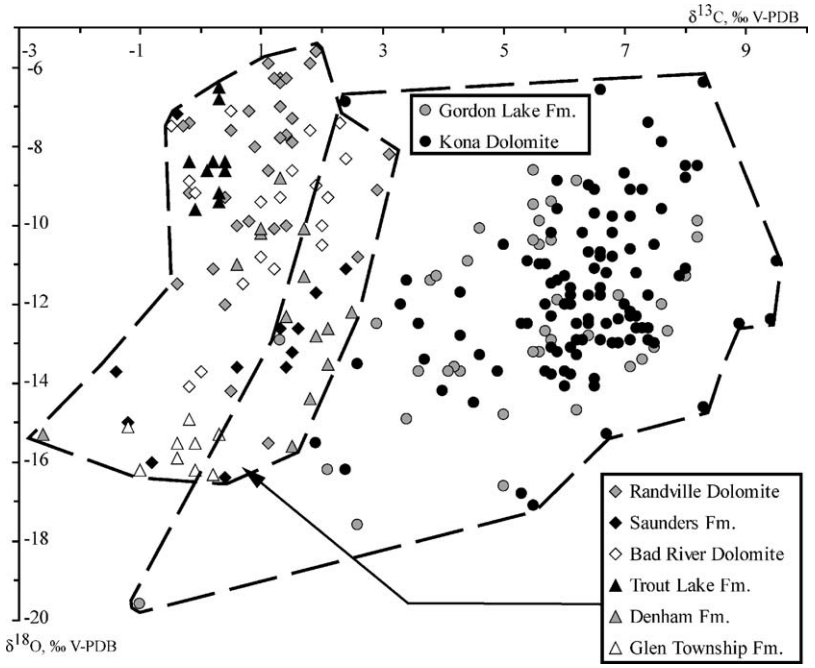


Fig. 8. $\delta^{18}O$ vs. $\delta^{13}C$ scatter diagram for studied Paleoproterozoic carbonates from the Great Lakes area.

carbonate recrystallization and significant depletion in $^{18}O$, samples in general were collected from thick siliciclastics-poor carbonate intervals that have been shown to preserve primary carbon isotope compositions during metamorphism (Wickham and Peters, 1993). Nevertheless, low $\delta^{18}O$ values and high Mn and Fe concentrations suggest equilibration with hot metamorphic or diagenetic fluids (Veizer, 1983). Similarly, low abundance of TOC and decreased fractionation between inorganic and organic carbon isotope compositions is likely related to metamorphic reequilibration of carbon, which can greatly alter $^{13}C$ abundances in TOC (Hayes et al., 1983). Therefore, some degree of $^{13}C$ depletion in carbonates may reflect either addition of newly formed phases with carbon derived from organic matter degradation or metamorphic devolatization. However, only metamorphism of siliceous carbonates can result in $^{13}C$ depletion of carbonate through Rayleigh distillation associated with decarbonation reactions (Valley, 1986; Baumgartner and Valley, 2001) and formation of certain metamorphic minerals (e.g. wollastonite). Lack of these minerals in our samples, which are predominantly pure carbonates, argues against a metamorphic explanation for low $\delta^{13}C$ values of carbonates from the Randville and Bad River dolomites, and Saunders, Trout Lake, Denham, and Glen Township formations with respect to carbonates of the Kona Dolomite and Gordon Lake Formation. Furthermore, mass balance considerations suggest that remineralization of organic matter in these organics-lean carbonates should not affect the $\delta^{13}C$ values by more than a per mil (cf. Pelechaty et al., 1996) and argue for a primary origin of these $\delta^{13}C$ values. Lastly, the general lack of correlation between $^{13}C$ abundances in these carbonates and those of $^{18}O$ (Fig. 8) or elemental concentrations (Table 1) support this notion. Accepting that carbon isotope abundances are generally well preserved in these carbonates, only the most altered samples of the Gordon Lake and Kona dolomites have similar $\delta^{13}C$ values to the most $^{13}C$-enriched carbonates from other studied units. Although facies variations in $\delta^{13}C$ compositions are possible, the magnitude of the carbon isotope difference between the Gordon Lake and Kona dolomites and other studied units is best explained by temporal differences.

### 5.2. *Climatic and tectonic setting in the aftermath of the Paleoproterozoic glacial epoch*

Insofar as carbonates in the Gordon Lake Formation and Kona Dolomite are geochemically distinct from post-glacial carbonates deposited in the western and southern parts of the Chocolay Basin, we conclude that these units were not contemporaneous. Either the western and southern carbonate successions are older, suggesting that they record seawater composition immediately after the last Huronian glacial event, or they are

younger, and record a negative $\delta^{13}C$ swing during the long-lived Lomagundi carbon isotope event.

To choose between these options, we first consider the climatic and tectonic setting for deposition of these carbonates in the aftermath of the Paleoproterozoic glacial epoch. All studied post-glacial Paleoproterozoic successions contain mature quartz sandstones either immediately above the youngest glacial diamictite or, if there is a break in deposition, immediately after deposition ensued (Table 3). These extremely thick and highly mature quartz sandstones were deposited in shallow depositional settings (Aspler et al., 1994; Chandler, 1984, 1986). Although often interpreted as indicators of extreme greenhouse conditions in the aftermath of icehouse conditions, their compositional maturity does increase upsection, suggesting that the degree of chemical weathering also increased with time (Young, 2004). Such thick and extensive quartz arenites are relatively rare in sedimentary record. The ~1.7 Ga Baraboo-Sioux-Barron quartz sandstones of the Lake Superior area and their correlatives in New Mexico, Arizona, Ontario, and Fennoscandia (Dott, 2003) and Early and Late Paleozoic quartz arenites are likely analogues to thick Paleoproterozoic post-glacial quartz arenites (Chandler, 1988a). These deposits were formed after the supercontinent assembly and the following orogenic collapse, rifting, and tectonic escape (Burke et al., 2003).

The origin of quartz arenite is generally related to intense weathering and associated with low relief, stable tectonic environment, low sedimentation rate, warm humid climate and, in some cases, eolian reworking (Johnsson et al., 1988; Chandler, 1988; Dott, 2003). Early Paleoproterozoic quartz sandstones were deposited in a range of depositional settings (Table 3); however, the presence of thin carbonate beds in these quartzites as well as pseudomorphs after gypsum and anhydrite in associated carbonates and argillites argues that climate was at least episodically arid.

The aftermath of the last Paleoproterozoic glaciation was marked by low relief continental landmasses and tectonic quiescence after the supercontinent assembly at 2.4 Ga (Barley et al., 2005; Fig. 9), collapse of orogens, and glacial leveling. High $pCO_2$ required to overcome the last Paleoproterozoic global glaciation contributed to warm climate since methane, a major Archean greenhouse gas, was unstable in the oxidized post-glacial atmosphere (Bekker et al., 2005). Post-glacial sea level rise increased precipitation inside the supercontinent; however low latitude position of landmasses enhanced tropical-style weathering, wind speed, and temperature gradient, resulting in dry continental climate inside the supercontinent. Apparent lag in compositional and chemical maturity of sandstones overlying the last Paleoproterozoic glacial diamictite with respect to the deglaciation likely reflects limits to the rate of chemical weathering despite high atmospheric $pCO_2$ level, rather than continuous rise of the $pCO_2$ in the aftermath of the Paleoproterozoic glacial epoch. The general absence of carbonates in the post-glacial interval is problematic given that seawater alkalinity should have been exceptionally high under such extreme weathering conditions. It may be that atmospheric and oceanic $CO_2$ and hence acidity was also extreme in the Huronian glacial aftermath, thereby preventing the wholesale deposition of shallow-water marine carbonates at that time (in stark contrast to Neoproterozoic post-glacial record).

### 5.3. Carbon isotope composition of seawater in the aftermath of the Paleoproterozoic glaciations

The beginning of the Lomagundi carbon isotope excursion is bracketed on the Fennoscandian Shield between the end of the Paleoproterozoic glacial epoch and the 2.22 Ga plume breakout event (Karhu and Holland, 1996). We have previously inferred (Bekker et al., 2003) that the early stage of this $\delta^{13}C$ excursion is marked by moderately $^{13}C$-enriched values based on limited carbon isotope data for thin carbonate beds associated with the horizon of enhanced chemical weathering below thick carbonate sequences with carbon isotope values >+4‰ typical for the Lomagundi carbon isotope excursion. Note that negative $\delta^{13}C$ values are the expected consequence of immediately post-glacial conditions, as noted in the middle Huronian Supergroup Espanola Formation (Bekker et al., 2005); these are not found above the youngest Paleoproterozoic glacial diamictite. Moderately to highly positive $\delta^{13}C$ values are recorded in the basal Gordon Lake Formation of the Huronian Supergroup, which is older than 2.22 Ga so it must preserve a record of the early part of the Lomagundi event. Here we accept that the thick evaporite-bearing Kona Dolomite of the Chocolay Group in Michigan is a direct correlative of the Gordon Lake Formation-based on the similarity of their carbon and sulfur isotope values (Cameron, 1983; Hemzacek et al., 1982; Hemzacek, 1987; Perry et al., 1984; Feng, 1986; Johnston et al., 2005; Table 4) and the presence of sulfate evaporites. If correct, the Kona Dolomite also records the onset of the Lomagundi excursion (Fig. 9).

Other thick carbonate units of the Chocolay Group previously believed to be broadly correlative with the Kona Dolomite (Fig. 2) show dramatically different carbon isotope compositions and notably lack evidence for evaporites, which are so prominent in both the Kona

Table 3
Depositional setting of mature quartz sandstones deposited in the aftermath of the Paleoproterozoic glacial epoch

| Name of the unit | Location | Thickness (m) | Depositional setting | Climate | References |
|---|---|---|---|---|---|
| Lorrain Formation | Ontario, Canada | 1500–3300 | Alluvial | Warm, relatively dry, seasonal | Chandler (1989) |
| Bar River Formation | Ontario, Canada | 300–900 | Shallow-marine | – | Chandler (1984) |
| Mesnard Quartzite | Marquette Range, Michigan, USA | 200 | Shallow-marine | – | Ojakangas et al. (2001) |
| Sturgeon Quartzite | Menominee and Iron River-Crystal Falls Ranges, WI and MI, USA | 100–600 | Shallow-marine | – | Ojakangas et al. (2001) |
| Sunday Quartzite | Gogebic Range, Wisconsin, USA | 50 | Shallow-marine | – | Ojakangas et al. (2001) |
| Medicine Peak Quartzite | Wyoming, USA | 1700 | Fluvial and deltaic | – | Karlstrom et al. (1983) |
| Sugarloaf Quartzite | Wyoming, USA | 580 | Shallow-marine | – | Karlstrom et al. (1983) |
| Maguse Member, Kinga Formation | Nunavut, Canada | 50–500 | Fluvial and eolian | Wet and warm, seasonal | Aspler and Chiarenzelli (1997) |
| Whiterock Member, Kinga Formation | Nunavut, Canada | 200–400 | Lacustrine | Wet, possibly equatorial | Aspler et al. (1994) |
| Jatulian Group | Karelia, Russia and Finland | 770–2500 | Fluvial and Lacustrine | – | Ojakangas et al. (2001a) |
| Dwaal Heuwel Formation | Transvaal Basin, South Africa | 30–120 | Shallow-marine | – | Button (1975) |
| Lucknow Formation/Mapedi Shale | Griqualand West Basin, South Africa | ~450 | Shallow-marine | – | Beukes and Smit (1987) |
| Cercadinho Formation | Quadrilátero Ferrífero, Brazil | ~317 | Shallow-marine | – | Bekker et al. (2003) |

Dolomite and Gordon Lake Formation. Therefore, these carbonates are either younger or older than the Kona Dolomite. During deposition of the Kona Dolomite, the shoreline was in the western part of the Marquette Trough (Taylor, 1972; Puffett, 1974; Gair, 1975), and likely did not extend to the Gogebic or Iron River Ranges. Therefore, unless other Chocolay Group carbonates accumulated in isolated depositional basins, they should be younger than the Kona Dolomite, reflecting subsequent transgression onto the continent. Abundant tidal signatures in all of the Chocolay Group mature quartz sandstones and the absence of interfingering facies expected in isolated depositional troughs argue for an open-marine setting that was set in a failed rift arm basin connected to the open ocean to the east. Consistent with this interpretation, paleocurrent measurements in the mature quartz sandstones are parallel to the embayment in Michigan and Wisconsin (Fig. 1; Pettijohn, 1957; Larue, 1981; LaBerge et al., 1992), but rotate to the south in the Huronian Basin (Pettijohn, 1957; Rousell and Long, 1998; Long, 2004) and there are significant local and regional variations in stratigraphic thickness (Larue, 1979). Sea level rise reflected by the transition from the shallow-marine Kona Dolomite to the conformably overlying Wewe Slate deposited below the wave base, which contains on the contact organic-rich pyriferous shale and mafic ash beds is plausibly related to basin deepening and reactivation that led to transgression onto the continent to the west.

In this interpretation, the events recorded by the Gordon Lake Formation in the Huronian Supergroup and the Kona Dolomite and the slightly younger carbonates of the Chocolay Group, imply that the early stage of the Lomagundi positive carbon isotope excursion was punctuated by the return to near 0‰ values prior to 2.22 Ga (Fig. 9). Consistent with this interpretation is the decrease in carbon isotope values at the top of the Kona Dolomite (Fig. 6).

On the other hand, carbonates of the Mille Lacs Group in central Minnesota occur in a stratigraphic succession lacking both glacial diamictite and mature quartz sandstone. The minimum $T_{DM}$ Sm–Nd age for this group is 2.07 Ga (Hemming et al., 1995) likely providing a maximum age for this group. Carbon isotope values of the Trout Lake, Denham, and Glen Township formations are near 0‰, which coupled with their age constraints are consistent with their deposition after the Lomagundi carbon isotope excursion (Fig. 9). Slightly $^{13}C$-enriched values of Denham dolomites might correspond to seawater composition at the end of the Lomagundi carbon isotope

Table 4
Sulfate evaporites in siliciclastic and carbonate successions deposited during the 2.22–2.1 Ga carbon isotope excursion

| Name of the unit | Location | Age (Ga) | Tectonic setting | Evaporite evidence | $\delta^{34}S$ values (‰ vs. CDT) | References |
|---|---|---|---|---|---|---|
| Gordon Lake Formation, Huronian Supergroup | North shore of Lake Huron, Ont., Canada | ca. 2.3–2.22 | Passive margin | Barite beds, silicified and pristine anhydrite and gypsum nodules and layers | +11.7–+15.6 | Cameron (1983), Chandler (1988), Bennett et al. (1989), this paper |
| Kona Dolomite, Chocolay Group | Marquette, MI, USA | ca. 2.3–2.22 | Intracratonic basin open to passive margin | Pseudomorphs after gypsum and anhydrite | +11.4–+16.0 | Taylor (1972), Clark (1974), Wohlabaugh (1980), Hemzacek et al. (1982), Hemzacek (1987), Perry et al. (1984), Feng (1986), this paper |
| Laparre Formation, Peribonca Group, Otish Supergroup | Otish Basin, Que., Canada | ca. 2.15 | Passive margin | Dolomite pseudomorphs after gypsum and anhydrite nodules and crystals | – | Genest (1985, 1989) |
| Lower part of the Nash Fork Formation, Snowy Pass Supergroup | Medicine Bow Mountains, WY, USA | ca. 2.15 | Passive margin | Molds after anhydrite nodules and gypsum crystals | – | Bekker and Eriksson (2003), Bekker et al. (2003) |
| Tulomozero Formation, Upper Jatulian Group | Lake Onega area, Karelia, Fennoscandian Shield, Russia | ca. 2.1 | Passive margin | Pseudomorphs after anhydrite and gypsum crystals and nodules | – | Akhmedov (1990), Ojakangas et al. (2001), Melezhik et al. (2005) |
| Lower Umba Formation, Lower Jatulian Group | Imandra-Varzuga Belt, Kola Peninsula, Russia | ca. 2.2 | Intracratonic rift basin | Barite beds | +27.8–+34.2 | Melezhik and Fetisova (1989), Grinenko et al. (1989) |
| Bubble Well Member, Juderina Formation, Yerrida Group | Nabberu Province, Western Australia | ca. 2.15 | Back-arc basin | Quartz pseudomorphs after gypsum and anhydrite | – | El Tabakh et al. (1999), Krapez and Martin (1999) |
| Lucknow Formation, Olifantshoek Group | South Africa | ca. 2.15 | Passive margin | Molds and quartz pseudomorphs after gypsum and anhydrite | – | Bekker et al. (2004a) |
| Norah Formation, Deweras Group | Magondi Belt, Zimbabwe | ca. 2.15 | Intracratonic rift basin | Layers of anhydrite | – | Master (1990) |
| Delwara Formation, Aravalli Group | Rajasthan, India | ca. 2.1 | Intracratonic rift basin | Barite layers | +17.1–+21.2 | Deb et al. (1991), Sreenivas et al. (2001) |
| Fedorovka Formation | Aldan Shield, Siberia, Russia | ca. 2.1 | Passive margin | Anhydrite layers and veins | up to +32.1 | Vinogradov et al. (1976), Zolotarev et al. (1989), Velikoslavinsky et al. (2003), Guliy and Wada (2003) |

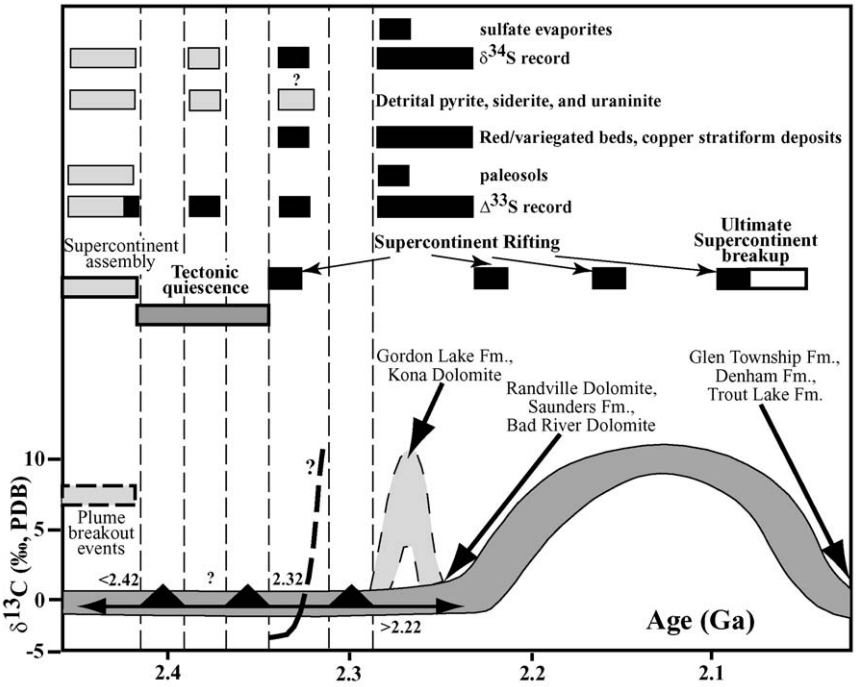


Fig. 9. Schematic representation of Paleoproterozoic secular carbon isotope variations after Bekker et al. (2005) with additional information from this paper shown in a light-grey pattern with a dashed border. Black triangles represent three Paleoproterozoic glaciations with their age constraints shown. Approximate age of the studied units is shown by arrows (see text for discussion). Tectonic events as well as indicators of atmospheric and ocean redox state relevant to this paper are from Bekker et al. (2005).

excursion since they are similar to those of dolomites of the Upper Nash Fork Formation in Wyoming (Bekker et al., 2003a), deposited immediately after the end of the ~2.22–2.1 Ga carbon isotope excursion.

### 5.4. Rise of seawater sulfate content associated with the early stage of the carbon isotope excursion

The general absence of sulfate casts in association with halite casts and carbonate deposits in shallow-marine Archean sedimentary successions (e.g. Eriksson et al., 2005) is consistent with low sulfate content in the Archean anoxic ocean. It is generally believed that sulfate evaporites were also absent in the Paleoproterozoic open-marine settings unless these were strongly affected by terrestrial runoff or were proximal to large igneous provinces (e.g. Pope and Grotzinger, 2003). Their absence in Paleoproterozoic and older sedimentary successions is attributed to either low atmospheric oxygen content or high bicarbonate saturation in seawater (Grotzinger and Kasting, 1993).

The early Paleoproterozoic rise of atmospheric oxygen and the initiation of the oxidative iron and sulfur cycles is recorded by the absence of non-mass-dependent sulfur isotope signals and highly negative $\delta^{34}S$ values of sedimentary sulfides and by the presence of associated hematitic pisolites and oölites that are sandwiched between diamictites of the Paleoproterozoic glacial epoch in South Africa (Bekker et al., 2004). Evidence for sulfate evaporites are unknown from this older stratigraphic level, and first appear in abundance during the Lomagundi event (Table 4). Deposition of these successions occurred in open-marine environments or in intracratonic rift or back-arc basins connected to the open ocean. Most of them are neither associated with nor in geographic proximity to large igneous provinces.

Insofar as the Kona Dolomite, Gordon Lake, and Peribonca formations (Table 4) are roughly similar in age, the aerial extent of sulfate evaporites may have reached over 1400 km along the margin of the Superior Craton (Chandler, 1988). Given our conclusion that both the Gordon Lake Formation and Kona Dolomite were deposited during the early stage of the Lomagundi carbon isotope excursion, the presence of the sulfate evaporites at this time constrains the rise of oceanic sulfate prior to 2.22 Ga. The rise of oceanic sulfate in association with the profound carbon isotope excursion is not unexpected since oxidative weathering linked to the high relative burial rate of organic matter and the rise of atmospheric oxygen would significantly enhance sulfate supply to the

ocean. Precipitation of halite after anhydrite or gypsum from evaporating seawater as recorded in some of these successions indicates that seawater sulfate levels were at or above 2.4 mmol (Holland, 2004), in contrast with modern levels of ~28 mmol.

Detailed study of subaqueous evaporite facies and collapse breccia of the ~1.88 Ga Stark Formation, Canada (Pope and Grotzinger, 2003) emphasized halite abundance while sulfate pseudomorphs were exceedingly rare. There are several units younger than 2.1 Ga but older than the Stark Formation that contain good evidence for sulfate evaporites. These include the ~1.9 Ga Tavani Formation, Hurwitz Group, Canada (Aspler and Chiarenzelli, 2002), ~2.0 Ga Kasegalik and McLeary formations, Belcher Islands, Canada (Bell and Jackson, 1974), and ~2.0 Ga Butin Formation, Siberia, Russia (Salop, 1982). Future work should resolve whether this difference reflects return after the Lomagundi event to less oxidized conditions in the ocean and, consequently, lower oceanic sulfate levels, which is consistent with the reappearance of BIFs at ~1.88 Ga (cf. Kump and Seyfried, 2005).

### 5.5. Tectonic evolution of the Great Lakes region between 2.5 and 2.0 Ga

Initiation of the Huronian Basin and deposition of the Chocolay Group was related to rifting of the Late Archean Kenorland supercontinent following tectonic quiescence on the Superior Craton since ~2.64 Ga (Young, 1988). However, in Western Australia and South Africa, the time period corresponding to the early stage in deposition of the Huronian Supergroup is marked by compressional tectonics culminating in deposition of the Turee Creek Group in a retroarc basin on the Pilbara Craton and folding and beveling on the Kaapvaal Craton (Krapez, 1996; Bekker et al., 2001 and references therein). Both successions deposited in compressional (e.g. Kaapvaal and Pilbara cratons) and extensional (e.g. Fennoscandian Shield and Superior Craton) settings were affected by the 2.5–2.4 Ga plume breakout events (Heaman, 1997, 2004; Fig. 9) and contain gigantic banded iron formations formed in open-marine settings (Barley et al., 1997; Isley and Abbott, 1999). Barley et al. (2005) suggested that assembly of the Late Archean supercontinent continued until ~2.40 Ga and that associated plume breakout events led to extension inside the assembled landmasses (Fig. 10A). Evidence for the Blezardian Orogeny bracketed in age between the 2477 ± 9 Ma Murray Granite (Krogh et al., 1996) and the two-phase 2415 ± 5 and 2376.3 ± 2.3 Ma Creighton Granite in the Huronian Basin (Riller and Schwerdtner, 1997; Riller et al., 1999; Smith, 2002) are consistent with the protracted supercontinent assembly. If this model is correct, extension and deposition of interlayered volcanic and siliciclastic sediments of the Lower Huronian Supegroup was initiated by the 2.5–2.4 Ga plume breakout events (Fig. 10A). Although rocks of this age are unknown in the Lake Superior area, detrital zircons of this age in the basal part of the Chocolay Group (Vallini et al., in press) indicate that rocks of this age were present in the source area and were eroded or are unrecognized today.

While three glaciations waxed and waned over the southern margin of the Superior Craton, only the youngest glacial event is recorded at the base of the Chocolay Group in Michigan to the west of the Huronian Basin (Fig. 10B and C). Ages of detrital zircon and hydrothermal xenotime constrain deposition of the Chocolay Group between 2298 ± 15 and 2207 ± 7 Ma (Vallini et al., in press). Transition from the rift to drift stage in the Huronian Basin is inferred to occur before the last glacial event, based on the Gowganda Formation stepping over older units on the Archean basement of the Superior Craton (Young, 1988). Tidal signatures are present only in the uppermost part of the Huronian Supergroup (Chandler, 1984; Rust and Shields, 1986) suggesting breakup on the eastern margin of the Superior Craton and connection to the ocean at about 2.3 Ga (Fig. 10C). Global tectonic significance of the ~2.3 Ga event is not clear but it likely initiated basins in which sediments of the Chocolay, Sarioli (Fennoscandia), lower part of the Hurwitz (Nunavut, Canada) and Pretoria (South Africa) groups were deposited. Mg-rich basalts with spinifex textures of the Sarioli Group and the 2295 ± 5 Ma Tulisaari dolerite dykes, Fennoscandia (Melezhik and Sturt, 1994; Hölttä et al., 2000) and the 2340 ± 7 Ma Thoa metagabbro on the western margin of the Rae Province, Canada (van Breemen and Bostock, 1994) might be related to plume breakout event or rifting at ~2.3 Ga. Needle-shaped detrital zircons of this age in diamictite and quartz sandstone of the Chocolay Group indicate mafic volcanism in the Lake Superior area during that time (Vallini et al., in press). Initiation of the Hurwitz deposition was however related to compressional (Andean-type volcanic arc) tectonic setting on the western margin of the Rae Province between 2.4 and 2.3 Ga (Hoffman, 1989; Bostock and van Breemen, 1994; Berman et al., 2004). The Huronian Supergroup was folded during the McGregor compressional phase prior to the intrusion of the 2.22 Ga Nipissing dykes and sills (Young, 1983). Assembly of the supercontinent associated with the plume breakout events could therefore continued until 2.3–2.22 Ga. Final breakup of the

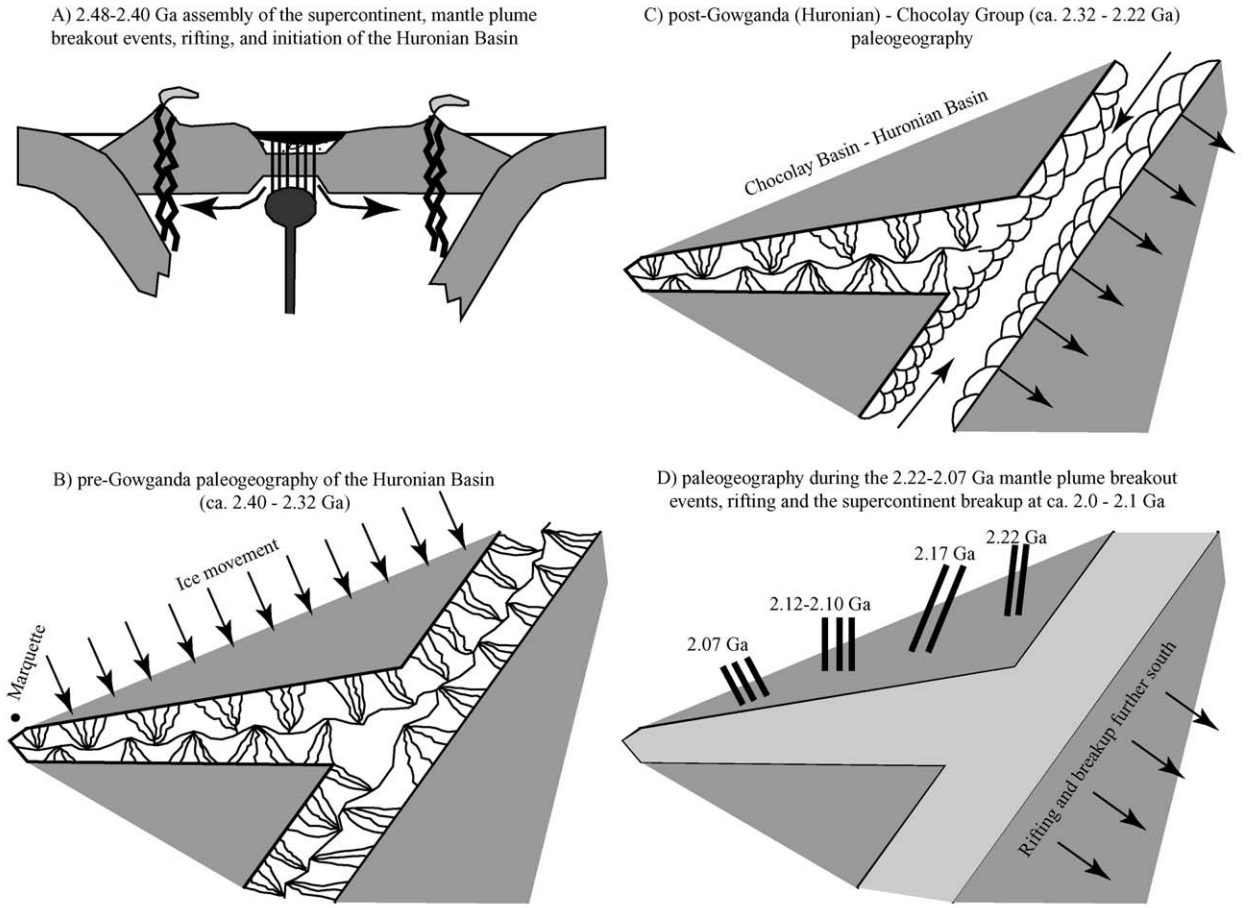


Fig. 10. Schematic paleogeography of the Huronian and Chocolay basins between 2.48 and 2.0 Ga. (A) Assembly of the supercontinent at ~2.48–2.40 Ga led to blanketing of mantle heat, plume breakout events, and associated rifting inside the supercontinent. The Huronian Basin as well as other Paleoproterozoic basins worldwide were initiated in this setting; (B) two oldest Huronian glaciations waxed and waned over the southern margin of the Superior Craton between ~2.40 and 2.32 Ga but left no trace in Michigan and Wisconsin; (C) renewed rifting and breakup to the east of the Huronian Basin at ~2.32 Ga and before deposition of the Gowganda Formation connected the Huronian Basin to the ocean while the Chocolay Group was deposited into an intracratonic basin. Note that the compressional McGregor-Michigan phase after deposition of the Chocolay and Huronian groups but before the 2.22 Ga Nipissing dykes and sills intruded is likely related to reversal to preceding extension along the southern margin of the Superior Craton and is broadly similar in age to the Ophthalmian and Eburnean orogenies in Western Australia and West Africa, respectively (Feybesse et al., 1998; Lahondère et al., 2002; Rasmussen et al., 2005); (D) several plume breakout events (2.22, 2.16, 2.12–2.10, and 2.07 Ga) affected the southern margin of the Superior Craton as well as other cratons worldwide. Finally, rifting and breakup at 2.1–2.0 Ga further south led to the passive margin setting along the southern margin of the Superior Craton which was overstepped and buried by foreland basin deposits. Note that retroarc basin developed at ~1.88 Ga within the failed rift arm into which the Chocolay Group was deposited.

Kenorland supercontinent was deferred until 2.1–2.0 Ga (Aspler and Chiarenzelli, 1998).

Following deposition of the Chocolay Group in an embayment formed by a failed rift arm extending to the passive margin to the east (Fig. 10C), several episodes of mafic igneous activity at ~2.21, 2.17, 2.12–2.10, and 2.08 Ga (progressively younging to the west) affected the southern margin of the Superior Craton (Halls and Davis, 2004; Fig. 10D). These episodes of mafic magmatism were felt on other cratons, and are most likely related to plume breakout events leading to rifting and, finally, breakup of the early Paleoproterozoic supercontinent. The last of these magmatic events in the Great Lakes region is reflected by the 2076 +5/−4 Ma Fort Frances tholeiitic dykes, which are plausibly linked to rifting and breakup along the southern margin of the Superior Province around 2.1 Ga. Fort Frances dykes might have been feeders to flood basalts that eroded prior to deposition of the Animikie Group (Southwick and Halls, 1987). Deposition of the Mille Lacs Group in a rift and passive margin setting might be also related to this event (Southwick and Day, 1983). Uplift, ero-

sion, and the initial phase of folding in the Mille Lacs Group may be related to a 10–15° counterclockwise rotation of the western Superior Province with respect to the eastern Superior Province along the Kapuskasing Zone at ~2.0 Ga (Halls and Davis, 2004). Sedimentary accumulation along the passive margin to the south of the depocenter of the early Paleoproterozoic basins in the Lake Superior area likely continued until formation around 1.88 Ga of an Andean-type volcanic arc with an associated retroarc basin into which the Menominee, Baraga, North Range, and Animikie groups were deposited (Fralick et al., 2002).

### 5.6. Implications for global correlation

New carbon and sulfur isotope data support correlation between the Gordon Lake Formation of the Huronian Supergroup and the Kona Dolomite of the Chocolay Group. Based on marked differences in $\delta^{13}C$ compositions and basin analysis, we suggest that the Randville and Bad River dolomites and the Saunders Formation are slightly younger than the Kona Dolomite and the correlative Gordon Lake Formation. Consistent with this interpretation is continuous deposition above the Gowganda Formation in the upper Huronian Supergroup and above the Enchantment Lake Formation of the Chocolay Group in the Marquette Trough whereas hiatus and paleosol separate the Fern Creek Formation and Sturgeon Quartzite in the Menominee Iron Range and glacial diamictite is entirely missing below the Bad River Dolomite in the Gogebic Range, WI where even the Sunday Quartzite disappears to the west (James et al., 1961; Schmidt, 1980; Ojakangas, 1997; LaBerge et al., 2003; Fig. 2). Carbonates and iron formations of the Mille Lacs Group are significantly younger than all these units, and were likely deposited at the end of the Lomagundi carbon isotope excursion.

Transgression at the base of the Wewe Slate in the Chocolay Basin might correspond with the transition from the sabkha to subaqueous storm-dominated shelf environment in the middle Gordon Lake Formation (Chandler, 1989) whereas the unconformity above the Bar River Quartzite of the Huronian Supergroup might correlate with the unconformity above the Wewe Slate and both might be related to the McGregor and correlative Michigan compressional phase (Young, 1983). Thicknesses of glacial diamictites, mature quartzites, and carbonates progressively decrease to the west with the exception of the Randville and Kona dolomites, which are much thicker than carbonates of the Gordon Lake Formation and the Sturgeon Quartzite, which is thicker than the Mesnard Quartzite (Larue, 1981). These data are consistent with the smaller accommodation space and delayed subsidence to the west.

Previously we proposed correlation between the Huronian Supergroup of North America and the Pretoria Group of South Africa (Bekker et al., 2001, 2005). In our scheme, the Gowganda and Timeball Hill-Makganyene glacial diamictites were considered time equivalents. This view was recently challenged by Hilburn et al. (2005) and Kopp et al. (2005) who suggest that the Timeball Hill-Makganyene glacial diamictites reflect a fourth Paleoproterozoic glacial event, which is unrecognized in North America. They proposed that oxygenic photosynthesis evolved after all Huronian glaciations and led to the oxidation of atmospheric methane and the only Paleoproterozoic 'Snowball Earth'. Kopp et al. (2005) specifically correlate the stratigraphic interval with the first evidence for the rise of atmospheric oxygen in South Africa (Rooihoogte and Timeball Hill formations; Bekker et al., 2004) with the post-Gowganda interval of the Huronian Supergroup that records lithologic and geochemical evidence for the rise of atmospheric oxygen (Bekker et al., 2001).

Insofar as lithologic evidence for four discrete Paleoproterozoic ice ages is lacking, we are skeptical of this interpretation (cf. Bekker, 2005), and find that it does not conform to the geological record. For example, if the interbasinal correlation by Kopp et al. (2005) were correct, mature quartzites should be found below the Timeball Hill and Makganyene glacial diamictites, but they are not. Furthermore, cap carbonates with negative carbon isotope values as in the Lower Duischland Formation (Bekker et al., 2001) should be above the Gowganda-equivalent glacial diamictites; these are absent. Finally, geochronologic constraints for the glacial diamictites in Michigan and Wisconsin bracket the third Huronian glaciation between $2288 \pm 15$ and $2217.5 \pm 1.6$ Ma (Fig. 11). Consequently, this North American ice age must be younger than the $2316 \pm 7$ Ma Rooihoogte-Lower Timeball Hill formations (Hannah et al., 2004), which are sandwiched between the two known South African glacial deposits of this era (Bekker et al., 2004). The minimum age for the South African ice ages is identical to that of the North American equivalents (Fig. 11) so we currently reject the idea of a fourth Paleoproterozoic glaciation.

With regard to the timing of glacial and magmatic events in South Africa, Altermann and Hälbich (1991) inferred a low-angle unconformity between the Makganyene Diamictite and the overlying 2.22 Ga Ongeluk Lava. Similarly, Hannah et al. (2004) suggested a time break between deltaic deposits of the Timeball Hill and Boshoek formations and subaerial volcanics of the

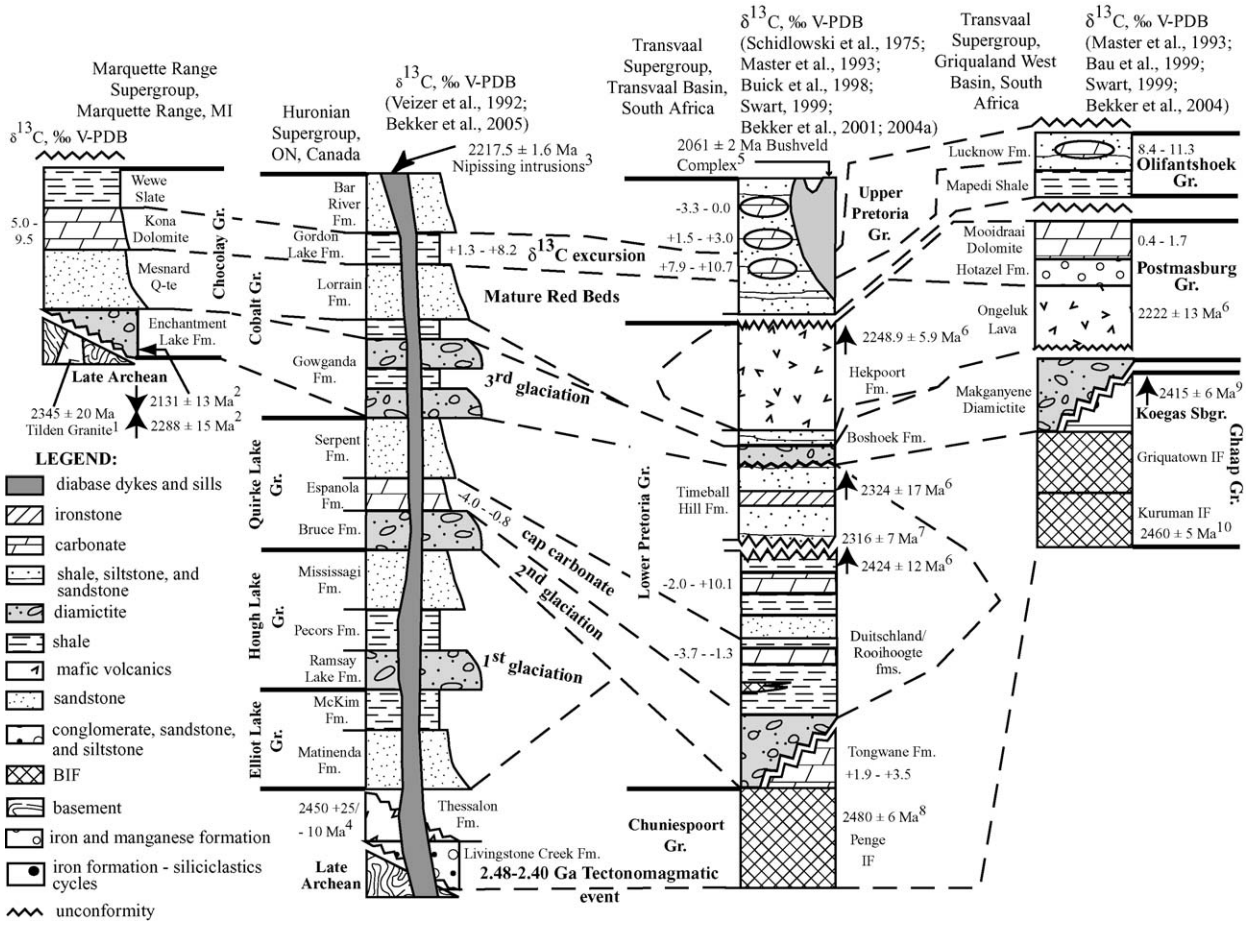


Fig. 11. Correlation chart for the Paleoproterozoic Chocolay Group, Michigan; Huronian Supergroup, Ontario; and Transvaal Supergroup of the Transvaal and Griqualand West basins, South Africa based on the 2.48–2.40 Ga tectonomagmatic event, three glaciations, cap carbonate above the middle glacial diamictite, mature red beds above the last glacial diamictite, geochronologic constraints, and >2.22–2.1 Ga carbon isotope excursion. References to age constraints—1: Hammond (1976); 2: Vallini et al. (in press); 3: Andrews et al. (1986); 4: Krogh et al. (1984); 5: Walraven (1997); 6: Dorland (2004); 7: Hannah et al. (2004); 8: Trendall unpubl. data in Nelson et al. (1999); 9: Gutzmer and Beukes (1998); 10: Pickard (2003). Age with an arrow pointing up indicates detrital zircon age (maximum age of deposition); age with an arrow pointing down indicates hydrothermal xenotime age (minimum age of deposition). Note that the Hekpoort Formation and Ongeluk Lava are correlative and close in age to the Nipissing diabase dykes and sills of the Huronian Basin (Buick et al., 1998; Master et al., 1993; Veizer et al., 1992; Schidlowski et al., 1975).

Hekpoort Formation. These interpretations consistently separate the timing of the last Paleoproterozoic ice age in South Africa and ~2.22 Ga plume breakout event. In our present interpretation, precipitation of Mn-oxides of the Hotozel Formation that directly overlies the Ongeluk Lava might reflect the rise of atmospheric oxygen during the ~2.22–2.1 Ga carbon isotope excursion (Karhu and Holland, 1996). Carbon isotope compositions of the overlying Mooidraai Dolomite are near to 0‰ (Bau et al., 1999; Swart, 1999; Fig. 11), which are similar to those of the Bad River and Randville dolomites and Saunders Formation in North America. Available geochronologic constraints are consistent with the correlation of these units (Fig. 11). If this correlation is correct, the long-lived Lomagundi event did contain at least one carbon isotope oscillation (cf. Melezhik et al., 1999). Given available geochronometric constraints, it is possible that the negative carbon isotope excursion during the Lomagundi anomaly might reflect a perturbation in the carbon cycle during the ~2.22 Ga plume breakout event.

## 6. Conclusions

The Gordon Lake Formation of the Huronian Supergroup and Kona Dolomite of the Chocolay Group overlie mature quartz sandstones and were deposited after the last Paleoproterozoic glaciation in North America at the onset of the Lomagundi (>2.22–2.1 Ga) carbon

isotope excursion. Carbonates in these units show $^{13}C$-enrichment up to +9.5‰ versus V-PDB and associated sulfates have similar $\delta^{34}S$ values ranging from +11.4 to +16.0‰ versus CDT. These are the oldest sedimentary sulfates and, therefore, they indicate that the rise of seawater sulfate content occurred at the early stage of the Lomagundi carbon isotope excursion in close association with the rise of atmospheric oxygen. Other carbonate units of the Chocolay Group (Bad River and Randville dolomites and Saunders Formation) preserved in separate structural basins in Michigan and Wisconsin, although considered to be lithostratigraphically correlative with these units, do not share the same level of $^{13}C$-enrichment. Based on basin analysis, we infer that they are slightly younger than the Gordon Lake Formation and Kona Dolomite and likely reflect perturbation in carbon cycle related to the ~2.22 Ga plume breakout event. Based on available geochronologic and chemostratigraphic constraints, we correlate these Chocolay Group carbonates with the Mooidraai Dolomite of the Postmasburg Group, South Africa. This correlation supports the view that there were only three global glaciations in the Paleoproterozoic Era.

The Chocolay Group was deposited after ~2.3 Ga in a failed rift arm open to the ocean on the east where the upper part of the Huronian Supergroup was deposited. Subsidence progressively expanded to the west and south, which is reflected by the similar lithostratigraphy but different chemostratigraphy of the Chocolay Group in separate structural basins in Michigan and Wisconsin. The following compressional stage led to the reversal in subsidence and left the >300 Ma long hiatus in deposition in the eastern part of the Great Lakes area. Carbonates of the Mille Lacs Group in Minnesota (Trout Lake, Glen Township, and Denham formations) have carbon isotope values close to 0‰ and were deposited during the rifting and breakup at 2.1–2.0 Ga further south along the southern margin of the Superior Craton. These units are the only remnants of the so far unrecognized tectonic event. Retroarc developed at ~1.9 Ga above the failed rift arm basin marking the transition from the passive to the Andean-type active margin.

Paleoproterozoic chemostratigraphy is still in a juvenile stage; although long-term trends are now established, shorter-term changes can only be constrained when detailed chemostratigraphic studies of sediments with low metamorphic grade are combined with precise geochronology. Our study highlights the strengths and limitations of the Paleoproterozoic record, and provides: (1) a model for evolution of Paleoproterozoic basins in the Great Lakes area, (2) new constraints for intra- and interbasinal correlations, (3) new insight into seawater compositions at the early stage of the most remarkable biogeochemical anomaly of the Paleoproterozoic Era, known as the Lomagundi event.

## Acknowledgements

This project started when AB was a M.S. student at the University of Minnesota, Duluth under the direction of R.W. Ojakangas. G. Bennett helped in field and with logistics. D. Rimstidt provided access to and helped with AAS work. Support came from Department of Geology, University of Minnesota, Duluth; GSA and southeastern section of GSA; Colorado Scientific Society; the graduate school and Department of Geological Sciences, VPI & SU; and, at the final stage, from NSF grant EAR-05-45484. Funding for participation by AJK and isotopic analyses at the University of Maryland was provided by NSF grants EAR-98-17348 and EAR-0126378 and NASA Exobiology grant NAG 512337. JAK thanks the Geological Survey of Finland for permission to publish data produced in their laboratories and A. Henttinen for assistance. Richard W. Ojakangas, Gene LeBerge, Gerry Bennett, and Ami Galarowicz provided initial samples for this work and information on geology of studied areas. Mark Severson pointed to drill cores of the Denham and Glen Township formations and clarified their geological setting. AB dedicates this paper to his brother Alexander Bekker who died in a car accident when this paper was written.

## References

Addison, W.D., Brumpton, G.R., Vallini, D.A., McNaughton, N.J., Davis, D.W., Kissin, S.A., Fralick, P.W., Hammond, A.L., 2005. Discovery of distal ejecta from the 1850 Ma Sudbury impact event. Geology 33, 193–196.

Akhmedov, A.M., 1990. Epochs of evaporization in the Paleoproterozoic of the Baltic Shield. Doklady Akademii Nauk 312 (3), 698–702.

Allen, R.C., 1910. The Iron River iron-bearing district of Michigan. Michigan Geol. Biol. Surv. Pub. 3, Geol. Ser. 2, 151 pp.

Altermann, W., Hälbich, I.W., 1991. Structural history of the southwestern corner of the Kaapvaal Craton and the adjacent Namaqua realm: new observations and a reappraisal. Precambrian Res. 52, 133–166.

Andrews, A.J., Masliwec, A., Morris, W.A., Owsiacki, L., York, D., 1986. The silver deposits at Cobalt and Gowganda, Ontario. II. An experiment in age determinations employing radiometric and paleomagnetic measurements. Can. J. Earth Sci. 23, 1507–1518.

Argast, A., 2002. The lower Proterozoic Fern Creek Formation, northern Michigan: mineral and bulk geochemical evidence for its glaciogenic origin. Can. J. Earth Sci. 39, 481–492.

Aspler, L.B., Chiarenzelli, J.R., 2002. Mixed siliciclastic-carbonate storm-dominated ramp in a rejuvenated Palaeoproterozoic intracratonic basin: upper Hurwitz Group, Nunavut, Canada. In: Altermann, W., Corcoran, P.L. (Eds.), Precambrian Sedimentary Envi-

ronments: A Modern Approach to Ancient Depositional Systems. Blackwell Science, pp. 293–321.

Aspler, L.B., Chiarenzelli, J.R., 1998. Two Neoarchean supercontinents? Evidence from the Paleoproterozoic. Sediment. Geol. 120, 75–104.

Aspler, L.B., Chiarenzelli, J.R., 1997. Initiation of ∼2.45–2.1 Ga intracratonic basin sedimentation of the Hurwitz Group, Keewatin Hinterland, Northwest Territories, Canada. Precambrian Res. 81, 265–297.

Aspler, L.B., Chiarenzelli, J.R., Bursey, T.L., 1994. Ripple marks in quartz arenites of the Hurwitz Group, Northwest Territories, Canada: evidence for sedimentation in a vast, Early Proterozoic, shallow, fresh-water lake. J. Sediment. Res. A 642, 282–298.

Barley, M.E., Bekker, A., Krapez, B., 2005. Late Archean to Early Paleoproterozoic global tectonics, environmental change and the rise of atmospheric oxygen. Earth Planet. Sci. Lett. 238, 156–171.

Barley, M.E., Pickard, A.L., Sylvester, P.J., 1997. Emplacement of a large igneous province as a possible cause of banded iron formation 2.45 billion years ago. Nature 385, 55–58.

Bau, M., Romer, R.L., Lüders, V., Beukes, N.J., 1999. Pb, O, and C isotopes in silicified Mooidraai dolomite (Transvaal Supergroup, South Africa): implications for the composition of Paleoproterozoic seawater and 'dating' the increase in oxygen in the Precambrian atmosphere. Earth Planet. Sci. Lett. 174, 43–57.

Baumgartner, L.P., Valley, J.W., 2001. Stable isotope transport and contact metamorphic fluid flow. Rev. Mineral. Geochem. 43, 415–467.

Bayley, R.W., Dutton, C.E., Lamey, C.A., 1966. Geology of the Menominee Iron-Bearing District Dickinson County, Michigan and Florence and Marinette Counties, Wisconsin with a section on the Carney Lake Gneiss by Trevis, S.B. U.S. Geol. Surv. Prof. Paper 513, p. 96.

Bayley, R.W., 1959. Geology of the Lake Mary Quadrangle, Iron County, Michigan. USGS Bull. 1077, 112 pp.

Beck, J.W., 1988. Implications for Early Proterozoic Tectonics and the Origin of Continental Flood Basalts, Based on Combined Trace Element and Neoymium/Strontium Isotopic Studies of Mafic Igneous Rocks of the Penokean, Lake Superior Belt, Minnesota, Wisconsin and Michigan. University of Minnesota, Minneapolis, 262 pp.

Bekker, A., 2005. Correlation of Paleoproterozoic glacial deposits: evidence for three global glaciations between 2.4 and 2.22 Ga. Earth System Processes 2, GSA Specialty Meetings, Abstracts with Programs, No. 1, p. 63.

Bekker, A., Eriksson, K.A., 2003. Paleoproterozoic drowned carbonate platform on the southeastern margin of the Wyoming Craton: a record of the Kenorland breakup. Precambrian Res. 120, 327–364.

Bekker, A., Kaufman, A.J., Karhu, J.A., Eriksson, K.A., 2005. Evidence for Paleoproterozoic cap carbonates in North America. Precambrian Res. 137, 167–206.

Bekker, A., Wang, P.-L., Rumble III, D., Stein, H.J., Hannah, J.L., Coetzee, L.L., Beukes, N.J., 2004. Dating the rise of atmospheric oxygen. Nature 427, 117–120.

Bekker, A., Holmden, C., Patterson, W., Eglington, B.L., Coetzee, L.L., Beukes, N.J., 2004a. Chemostratigraphy of early Paleoproterozoic carbonates of South Africa. GSA Abstr. Programs 36 (6), 341.

Bekker, A., Sial, A.N., Karhu, J.A., Ferrerira, V.P., Noce, C.M., Kaufman, A.J., Romano, A.W., Pimentel, M.M., 2003. Chemostratigraphy of carbonates from the Minas Supergroup, Quadrilátero Ferrífero (Iron Quadrangle), Brazil: a stratigraphic record of early Proterozoic atmospheric, biogeochemical and climatic change. Am. J. Sci. 303, 865–904.

Bekker, A., Karhu, J.A., Eriksson, K.A., Kaufman, A.J., 2003a. Chemostratigraphy of Paleoproterozoic carbonate successions of the Wyoming Craton: tectonic forcing of biogeochemical change? Precambrian Res. 120, 279–325.

Bekker, A., Kaufman, A.J., Karhu, J.A., Beukes, N.J., Swart, Q.D., Coetzee, L.L., Eriksson, K.A., 2001. Chemostratigraphy of the Paleoproterozoic Duitschland Formation, South Africa: implications for coupled climate change and carbon cycling. Am. J. Sci. 301, 261–285.

Bell, R.T., Jackson, G.D., 1974. Aphebian halite and sulphate indications in the Belcher Group, Northwest Territories. Can. J. Earth Sci. 11, 722–728.

Bennett, G., Dressler, B.O., Robertson, J.A., 1991. The Huronian Supergroup and associated intrusive rocks. In: Thurston, P.C., Williams, H.R., Sutcliffe, R.H., Stott, G.M. (Eds.), Geology of Ontario. Ontario Geological Survey Special Volume 4, Part 1, Toronto, pp. 549–591.

Bennett, G., Born, P., Hatfield, K., 1989. A report on a recently identified dolostone unit in Fenwick Township, Goulais Bay area, District of Algoma. In: Fenwick, K.G., Giblin, P.E., Pitts, A.E. (Eds.), Report of activities 1988. Resident Geologists, Ontario Geological Survey Miscellaneous Paper 142, pp. 211–215.

Berman, R.G., Sanborn-Barrie, M., Stern, R.A., Jercinovic, M.J., Skulski, T., 2004. Collisional orogenesis at ca. 2.35 Ga in the Rae Domain, Western Churchill Province, Nunavut, Canada. GSA Abstracts with Programs 36 (6), 255–256.

Beukes, N.J., Smit, C.A., 1987. New evidence for thrust faulting in Griqualand West, South Africa: implications for stratigraphy and the age of red beds. S. Afr. J. Geol. 90 (4), 378–394.

Boerboom, T.J., Jirsa, M.A., 2001. Stratigraphy of the Paleoproterozoic Denham Formation—a continental margin assemblage of basalt, arkose, and dolomite. In: Institute on Lake Superior Geology Proceedings, 47th Annual Meeting, vol. 47, No. 1, pp. 6–7 (abstract).

Boerboom, T.J., Southwick, D.L., Severson, M.J., 1999. Geological map of the Mille Lacs Lake 30 × 60 min Quadrangle, East-Central Minnesota. Minnesota Geological Survey Miscellaneous Map Series M-100, Plate 1, Scale 1:100,000.

Bostock, H.H., van Breemen, O., 1994. Ages of detrital and metamorphic zircons and monazites from a pre-Taltson magmatic zone basin at the western margin of Rae Province. Can. J. Earth Sci. 31, 1353–1364.

Buchan, K.L., Halls, H.C., Mortensen, J.K., 1996. Paleomagnetism, U–Pb geochronology, and geochemistry of Marathon dykes, Superior Province, and comparison with the Fort Frances swarm. Can. J. Earth Sci. 33, 1583–1595.

Buick, I.S., Uken, R., Gibson, R.L., Wallmach, T., 1998. High-$\delta^{13}$C Paleoproterozoic carbonates from the Transvaal Supergroup, South Africa. Geology 26, 875–878.

Burke, K., MacGregor, D.S., Cameron, N.R., 2003. Africa's petroleum systems; four tectonic 'Aces' in the past 600 million years. In: Arthur, T.J., MacGregor, D.M., Cameron, N.R. (Eds.), Petroleum Geology of Africa: New Themes and Developing Technologies, vol. 207. Geological Society, London, pp. 21–60 (Special Publications).

Button, A., 1975. A palaeocurrent study of the Dwaal Heuvel Formation, Transvaal Supergroup. Trans. Geol. Soc. S. Afr. 78, 173–183.

Cameron, E.M., 1983. Evidence from early Proterozoic anhydrite for sulfur isotopic partitioning in Precambrian oceans. Nature 304, 54–56.

Cannon, W.F., 1980. Copper-bearing quartzite near Watersmeet, Michigan. U.S. Geol. Surv. Open-File Report 80-390, 6 pp.

Card, K.D., 1978. Metamorphism of the Middle Precambrian (Aphebian) rocks of the eastern southern province, Metamorphism in the Canadian Shield. Geol. Surv. Can., 269–282, Paper 78-10.

Chandler, F.W., 1989. Lower Proterozoic sabkha-related copper mineralization, paleoenvironment and diagenesis, Cobre Lake, Ontario. In: Boyle, R.W., Brown, A.C., Jefferson, C.W., Jowett, E.C., Kirkham, R.V. (Eds.), Sediment-hosted Stratiform Copper Deposits. Geological Association, Canada, pp. 225–244.

Chandler, F.W., 1988. Diagenesis of sabkha-related, sulphate nodules in the Early Proterozoic Gordon Lake Formation, Ontario, Canada. Carbonate Evaporite 3 (1), 75–94.

Chandler, F.W., 1988a. Quartz arenites: review and interpretation. Sed. Geol. 58, 105–126.

Chandler, F.W., 1986. Sedimentology and paleoclimatology of the Huronian (Early Aphebian) Lorrain and Gordon Lake Formations and their bearing on models for sedimentary copper mineralization, Current Research, Part A. Geological Survey of Canada, Paper 86-1A, pp. 121–132.

Chandler, F.W., 1984. Sedimentary setting of an Early Proterozoic copper occurrence in the Cobalt Group, Ontario: a preliminary assessment, Current Research, Part A. Geological Survey of Canada, Paper 84-1A, pp. 185–192.

Clark, J.L., 1974. Sulfide mineralization in the Kona Dolomite, Marquette County, Michigan. M.Sc. Thesis. Michigan Technological University, Houghton, MI, 49 pp.

Clements, J.M., Smyth, H.L., 1899. The Crystal Falls iron-bearing district of Michigan. U.S. Geol. Surv. 19th Ann. Rept., pt. 3, pp. 1–151.

Deb, M., Hoefs, J., Baumann, A., 1991. Isotopic composition of two Precambrian stratiform barite deposits from the Indian shield. Geochim. Cosmochim. Acta 55, 303–308.

Dorland, H.C., 2004. Provenance ages and timing of sedimentation of selected Neoarchean and Paleoproterozoic successions on the Kaapvaal Craton. Ph.D. Thesis. Rand Afrikaans University, Johannesburg, South Africa, 326 pp.

Dott Jr., R.H., 2003. The importance of eolian abrasion in supermature quartz sandstones and the paradox if weathering on vegetation-free landscapes. J. Geol. 111, 387–405.

Eldougdoug, A.A., 1984. Petrology and geochemistry of the volcanosedimentary Glen Township Formation, Aitkin County, east-central Minnesota: implications for gold exploration. Ph.D. Thesis. University of Minnesota, Minneapolis, 199 pp.

El Tabakh, M., Grey, K., Pirajno, F., Schreiber, B.C., 1999. Pseudomorphs after evaporitic minerals interbedded with 2.2 Ga stromatolites of the Yerriba basin, Western Australia: origin and significance. Geology 27 (10), 871–874.

Eriksson, K.A., Simpson, E.L., Master, S., Henry, G., 2005. Neoarchaean (ca. 2.58 Ga) halite casts: implications for palaeoceanic chemistry. J. Geol. Soc. London 162, 789–799.

Feng, J., 1986. Sulfur and Oxygen Isotope Geochemistry of Precambrian Marine Sulfate and Chert. Northern Illinois University, Dekalb, 110 pp.

Feybesse, J.L., Johan, V., Triboulet, C., Guerrot, C., Mayaga-Mikolo, F., Bouchot, V., Eco N'dong, J., 1998. The West Central African belt: a model of 2.5–2.0 Ga accretion and two-phase orogenic evolution. Precambrian Res. 87, 161–216.

Fralick, P., Davis, D.W., Kissin, S.A., 2002. The age of the Gunflint Formation, Ontario, Canada: single zircon U–Pb age determinations from reworked volcanic ash. Can. J. Earth Sci. 39, 1085–1091.

Fralick, P.W., Miall, A.D., 1989. Sedimentology of the Lower Huronian Supergroup (Early Proterozoic), Elliot Lake area, Ontario, Canada. Sed. Geol. 63, 127–153.

Frarey, M.J., 1985. Proterozoic geology of the Lake Panache-Collins Inlet area, Ontario. Geological Survey of Canada, Paper 83-22, Ottawa, 61 pp.

Gair, J.E., 1975. Bedrock geology and ore deposits of the Palmer Quadrangle, Marquette County, Michigan. U.S. Geol. Surv. Prof. Paper 769, 159 pp.

Gair, J.E., Thaden, R.E., 1968. Geology of the Marquette and Sands Quadrangles Marquette County Michigan. US Geol. Surv. Prof. Paper 397, 77 pp.

Gair, J.E., Wier, K.L., 1956. Geology of the Kiernan Quadrangle, Iron County, Michigan. USGS Bull., 1044, 88 pp.

Genest, S., 1989. Analyse du bassin d'Otish (Protérozoïque inférieur, Québec). Ph.D. Thesis. Université de Montéal, Montéal, 336 pp.

Genest, S., 1985. Aphebian evaporites and related red beds in the Peribonca Formation (Otish Group, Central Quebec): evidence for coastal sabkha and subaqueous environments. GAC/MAC Programs with abstracts, No. 10, p. A21.

Giblin, P.E., Leahy, E.J., Robertson, D.W., 1976. Sault Ste. Marie-Elliot Lake. Ontario Geological Survey, Geological Compilation Series, Map 2419, scale 1:25,000.

Goldich, S.S., Fischer, L.B., 1986. Air-abrasion experiments in U–Pb dating of zircon. Chem. Geol. 58, 195–215.

Grassineau, N.V., Mattey, D.P., Lowry, D., 2001. Sulfur isotope analysis of sulfide and sulfate minerals by continuous flow-isotope ratio mass spectrometry. Anal. Chem. 73, 220–225.

Greenman, N.N., 1951. The origin of the Randville Dolomite of Dickinson and Iron Counties, Michigan. Ph.D. Thesis. University of Chicago, Chicago, 179 pp.

Grinenko, L.N., Melezhik, V.A., Fetisova, O.A., 1989. First discovery of barites in the Precambrian sedimentary deposits of Baltic Shield. Doklady Akademii Nauk 304 (6), 1453–1455 (in Russian).

Grotzinger, J.P., Kasting, J.F., 1993. New constraints on Precambrian ocean composition. J. Geol. 101, 235–243.

Guliy, V.N., Wada, H., 2003. Macro- and microvariations of isotopic composition of carbon and oxygen of carbonates from the Precambrian of the Aldan Shield. Geokhimiya (5), 482–491.

Gutzmer, J., Beukes, N.J., 1998. High grade manganese ores in the Kalahari manganese field: characterization and dating of the ore-forming events. Unpublished Report. Rand Afrikaans University, Johannesburg, 221 pp.

Halls, H.C., Davis, D.W., 2004. Paleomagnetism and U–Pb geochronology of the 2.17 Ga Biscotasing dyke swarm, Ontario, Canada: evidence for vertical-axis crustal rotation across the Kapuskasing Zone. Can. J. Earth Sci. 41, 255–269.

Hammond, R.D., 1976. Geochronology and origin of Archean rocks in Marquette County, Upper Michigan. M.S. Thesis. University of Kansas, Lawrence, 108 pp.

Hannah, J.L., Bekker, A., Stein, H.J., Markey, R.J., Holland, H.D., 2004. Primitive Os and 2316 Ma age for marine shale: implications for Paleoproterozoic glacial events and the rise of atmospheric oxygen. Earth Planet. Sci. Lett. 225, 43–52.

Hayes, J.M., Kaplan, I.R., Wedeking, K.W., 1983. Precambrian organic geochemistry, preservation of the record. In: Schopf, J.W. (Ed.), The Earth's Earliest Biosphere: Its Origin and Evolution. Princeton University Press, Princeton, NJ, pp. 93–134.

Heaman, L.M., 2004. 2.5–2.4 Ga global magmatism: remnants of supercontinents or products of superplumes? GSA Abstracts with Programs 36 (6), 255.

Heaman, L.M., 1997. Global mafic volcanism at 2.45 Ga: remnants of an ancient large igneous province? Geology 25, 299–302.

Heaman, L.M., Easton, R.M., 2005. Proterozoic history of the Lake Nipigon area, Ontario: constraints from U–Pb zircon and badde-

leyite dating. In: Institute on Lake Superior Geology Proceedings, 51st Annual Meeting, vol. 51, No. 1, pp. 24–25 [abstract].

Hemming, S.R., Hanson, G.N., McLennan, S.M., 1995. Precambrian crustal blocks in Minnesota-Neodymium isotope evidence from basement and metasedimentary rocks. In: Sims, P.K., Carter, L.M.H. (Eds.), US Geol. Surv. Bull. 1904. Contributions to Precambrian Geology of Lake Superior Region, pp. U1–U15.

Hemzacek, J.M., 1987. Replaced evaporites and the sulfur isotope age curve of the Precambrian. M.Sc. Thesis. Northern Illinois University, Dekalb, IL, 77 pp.

Hemzacek, J.M., Perry, E.C., Larue, D.K., Feng, J., 1982. Sulfur isotope composition of sulfate in chert horizons of the Proterozoic (Precambrian X) Kona Dolomite, Marquette Region, Michigan. GSA Abstracts with Programs 14 (7), 512.

Hilburn, I.A., Kirschvink, J.L., Tajika, E., Tada, R., Hamano, Y., Yamamoto, S., 2005. A negative fold test on the Lorrain Formation of the Huronian Supergroup: uncertainty on the paleolatitude of the Paleoproterozoic Gowganda glaciation and implications for the great oxidation event. Earth Planet. Sci. Lett. 232, 315–332.

Hofmann, H.J., Pearson, D.A.B., Wilson, B.H., 1980. Stromatolites and fenestral fabric in Early Proterozoic Huronian Supergroup, Ontario. Can. J. Earth Sci. 17, 1351–1357.

Hoffman, P.F., 1989. Precambrian geology and tectonic history of North America. In: Bally, A.W., Palmer, A.R. (Eds.), The Geology of North America. Geological Society of America, pp. 447–511.

Holland, H.D., 2004. The geological history of seawater. In: Holland, H.D., Turekian, K.K. (Eds.), Treatise on Geochemistry. Elsevier, Oxford, pp. 583–625.

Holm, D.K., 1986. A structural investigation and tectonic interpretation of the Penokean orogeny: East-Central Minnesota. M.Sc. Thesis. University of Minnesota, Duluth, 114 pp.

Holm, D.K., Van Schmus, W.R., MacNeill, L.C., Boerboom, T.J., Schweitzer, D., Schneider, D.A., 2005. U–Pb geochronology of Paleoproterozoic plutons from the northern midcontinent, USA: evidence for subduction flip and continued convergence after geon 18 Penokean orogenesis. GSA Bull. 117 (3/4), 259–275.

Hölttä, P., Huhma, H., Mänttäri, I., Paavola, J., 2000. *P–T–t* development of Archaean granulites in Varpaisjärvi, Central Finland II. Dating of high-grade metamorphism with the U–Pb and Sm–Nd methods. Lithos 50, 121–136.

Isley, A.E., Abbott, D.H., 1999. Plume-related mafic volcanism and the deposition of banded iron formation. J. Geophys. Res. 104 (B7), 15461–15477.

Jackson, S.L., 1994. Geology of the Aberdeen Area. Open File Report 5903, Ontario Geological Survey, 69 pp.

James, H.L., Dutton, C.E., Pettijohn, F.J., Wier, K.L., 1968. Geology and ore deposits of the Iron River-Crystal Falls District, Iron County Michigan. U.S. Geol. Surv. Prof. Paper 570, 134 pp.

James, H.L., Clark, L.D., Lamey, C.A., Pettijohn, F.J., Freedman, J., Trow, J., Wier, K.L., 1961. Geology of Central Dickinson County, Michigan. U.S. Geol. Surv. Prof. Paper 310, 176 pp.

James, H.L., 1955. Zones of regional metamorphism in the Precambrian of northern Michigan. Geol. Soc. Am. Bull. 66 (12), 1455–1488.

Johnsson, M.J., Stallard, R.F., Meade, R.H., 1988. First-cycle quartz arenites in the Orinoco River Basin, Venezuela and Colombia. J. Geol. 96 (3), 263–277.

Johnston, D.T., Wing, B.A., Farquhar, J., Kaufman, A.J., Strauss, H., Lyons, T.W., Kah, L.C., Canfield, D.E., 2005. Active microbial sulfur disproportionation in the Mesoproterozoic. Science 310, 1477–1479.

Karhu, J.A., Holland, H.D., 1996. Carbon isotopes and the rise of atmospheric oxygen. Geology 24 (10), 867–870.

Karlstrom, K.E., Flurkey, A.J., Houston, R.S., 1983. Stratigraphy and depositional setting of the Proterozoic Snowy Pass Supergroup, southeastern Wyoming: record of a Paleoproterozoic Atlantic-type cratonic margin. Geol. Soc. Am. Bull. 94, 1257–1274.

Komatar, F.D., 1972. Geology of the Animikian metasedimentary rocks, Mellen Granite, and Mineral Lake Gabbro west of Mellen, Wisconsin. M.Sc. Thesis. University of Wisconsin, Madison, 70 pp.

Kopp, R.E., Kirschvink, J.L., Hilburn, I.A., Nash, C.Z., 2005. The Paleoproterozoic snowball Earth: a climate disaster triggered by the evolution of oxygenic photosynthesis. Proc. Natl. Acad. Sci. 102 (32), 11131–11136.

Krapez, B., 1996. Sequence-stratigraphic concepts applied to the identification of basin-filling rhythms in Precambrian successions. Aust. J. Earth Sci. 43, 355–380.

Krapez, B., Martin, D.M., 1999. Sequence stratigraphy of the Paleoproterozoic Nabberu Province of Western Australia. Aust. J. Earth Sci. 46, 89–103.

Krogh, T.E., Kamo, S.L., Bohor, B.F., 1996. Shock metamorphosed zircons with correlated U–Pb discordance and melt rocks with concordant protolith ages indicate an impact origin for the Sudbury structure, Earth Processes: reading the isotopic code. Geophys. Monograph 95. Am. Geophys. Union, pp. 343–353.

Krogh, T.E., Davis, D.W., Corfu, F., 1984. Precise U–Pb zircon and badelleyite ages for the Sudbury area. In: Pye, E.G., Naldrett, A.J., Giblin, P.E. (Eds.), The Geology and Ore Deposits of the Sudbury Structure, 1. Ontario Geol. Surv. Spec., pp. 431–446.

Kump, L.R., Seyfried Jr., W.E., 2005. Hydrothermal Fe fluxes during the Precambrian: effect of low oceanic sulfate concentrations and low hydrostatic pressure on the composition of black smokers. Earth Planet. Sci. Lett. 235, 654–662.

LaBerge, G.L., Klasner, J.S., Cannon, W.F., Ojakangas, R.W., 2003. Field trip 2: Menominee Iron District. In: Proceedings of the 49th Annual Meeting of Institute on Lake Superior Geology, vol. 49, Part 2: Field Trip Guidebook, Iron Mountain, MI, pp. 48–63.

LaBerge, G.L., Ojakangas, R.W., Licht, K.J., 1992. Archean and Early Proterozoic geology of the Gobebic District, Northern Michigan and Wisconsin. In: Proceedings and Abstracts, Annual Meeting, Institute on Lake Superior Geology, vol. 38, Part 2: Field Trip Guidebook, Hurley, WI, 40 pp.

Lahondère, D., Thiéblemont, D., Tegyey, M., Guerrot, C., Diabate, B., 2002. First evidence of early Birimian (2.21 Ga) volcanic activity in Upper Guinea: the volcanics and associated rocks of the Niani suite. J. Afr. Earth Sci. 35, 417–431.

Larue, D.K., 1981. The Chocolay Group, Lake Superior region, U.S.A.: sedimentologic evidence for deposition in basinal and platform settings on an early Proterozoic craton. GSA Bull. 92, 417–435.

Larue, D.K., 1979. Sedimentary history prior to chemical iron sedimentation of the Precambrian X Chocolay and Menominee groups (Lake Superior Region). Ph.D. Thesis. Northwestern University, Evanston, 171 pp.

Leith, C.K., 1925. Silicification of erosion surfaces. Econ. Geol. 20 (6), 513–523.

Long, D.G.F., 2004. The tectonostratigraphic evolution of the Huronian basement and the subsequent basin fill: geological constraints on impact models of the Sudbury event. Precambrian Res. 129, 203–223.

Long, D.G.F., Young, G.M., Rainbird, R.H., Fedo, C.M., 1999. Actualistic and non-actualistic Precambrian sedimentary styles: examples from the Proterozoic, north shore of Lake Huron. Field Trip B5

Guidebook. In: Proceedings of the Joint Annual Meeting of Geological Association of Canada–Minnesota Association of Canada, 50 pp.

Marsden, R.W., 1972. Cuyuna district. In: Sims, P.K., Morey, G.B. (Eds.), Geology of Minnesota: A Centennial Volume. Minnesota Geological Survey, St. Paul, pp. 227–239.

Master, S., Verhagen, B.T., Bassot, J.P., Beukes, N.J., Lemoine, S., 1993. Stable isotopic signatures of Paleoproterozoic carbonate rocks from Guinea, Sinegal, South Africa and Zimbabwe: constrains on the timing of the ca. 2 Ga "Lomagundi" $\delta^{13}C$ excursion, Symposium: early Proterozoic geochemical and structural constraints–metallogeny: Publication Occasionnelle 1993/23, pp. 38–41, Dacar, Sénégal.

Master, S., 1990. Oldest evaporites in Africa: 2.06 Ga continental playa deposits of the Deweras Group, Zimbabwe. In: Proceedings of the 15th Colloquium of African Geology. Universite Nancy I, 103 pp.

Melezhik, V.A., Fallick, A.E., 1996. A widespread positive $\delta^{13}C_{carb}$ anomaly at around 2.33–2.06 Ga on the Fennoscandian Shield: a paradox? Terra Nova 8, 141–157.

Melezhik, V.A., Fallick, A.E., Rychanchik, D.V., Kuznetsov, A.B., 2005. Paleoproterozoic evaporites in Fennoscandia: implications for seawater sulfate, the rise of atmospheric oxygen and local amplification of the $\delta^{13}C$ excursion. Terra Nova 17, 141–148.

Melezhik, V.A., Fallick, A.E., Medvedev, P.V., Makarikhin, V.V., 1999. Extreme $\delta^{13}C_{carb}$ enrichment in ca. 2.0 Ga magnesite-stromatolite-dolomite-'red beds' association in a global context: a case for the world-wide signal enhanced by a local environment. Earth Sci. Rev. 48, 71–120.

Melezhik, V.A., Sturt, B.A., 1994. General geology and evolutionary history of the early Proterozoic Polmak-Pasvik-Pechenga-Imandra/Varzuga-Ust Ponoy Greenstone Belt in the northeastern Baltic Shield. Earth Sci. Rev. 36, 205–241.

Melezhik, V.A., Fetisova, O.A., 1989. First discovery of syngenetic barites in the Precambrian of the Baltic Shield. Doklady Akademii Nauk 307 (2), 422–425 (in Russian).

Morey, G.B., 1996. Continental margin assemblage. In: Sims, P.K., Carter, L.M.H. (Eds.), Archean and Proterozoic Geology of the Lake Superior Region, U.S.A., 1993, U.S. Geological Survey Professional Paper 1556. United States Government Printing Office, Washington, pp. 30–44.

Morey, G.B., 1978. Lower and middle Precambrian stratigraphic nomenclature for east-central Minnesota, Minnesota Geological Survey. Report of Investigations 21, University of Minnesota, Saint Paul, 52 pp.

Morey, G.B., 1972. General geological setting. In: Sims, P.K., Morey, G.B. (Eds.), Geology of Minnesota: A Centennial Volume. Minnesota Geological Survey, St. Paul, pp. 199–203.

Morey, G.B., Southwick, D.L., 1995. Allostratigraphic relationships of early Proterozoic iron-formations in the Lake Superior region. Econ. Geol. 90, 1983–1993.

Nelson, D.R., Trendall, A.F., Altermann, W., 1999. Chronological correlations between the Pilbara and Kaapvaal cratons. Precambrian Res. 97, 165–189.

Ojakangas, R.W., 1997. Correlative sequence within the Marquette Range Supergroup (Michigan) and the Huronian Supergroup (Ontario); Glaciogenics, paleosols, and orthoquartzites (Abs), 43rd Inst. Lake Superior Geol., pp. 47–48.

Ojakangas, R.W., Morey, G.B., Southwick, D.L., 2001. Paleoproterozoic basin development and sedimentation in the Lake Superior region, North America. Sed. Geol. 141/142, 319–341.

Ojakangas, R.W., Marmo, J.S., Heiskanen, K.I., 2001a. Basin evolution of the Paleoproterozoic Karelian Supergroup of the Fennoscandian (Baltic) Shield. Sed. Geol. 141/142, 255–285.

Panahi, A., Young, G.M., Rainbird, R.H., 2000. Behaviour of major and trace elements (including REE) during Paleoproterozoic pedogenesis and diagenetic alteration of an Archean granite near Ville Marie, Quebec, Canada. Geochim. Cosmochim. Acta 64, 2199–2220.

Pearson, W.N., 1979. Copper metallogeny, North shore region of Lake Huron, Ontario. Current Research, Part A, Geol. Surv. Can. (Paper 79-1A), pp. 289–304.

Pelechaty, S.M., Kaufman, A.J., Grotzinger, J.P., 1996. Evaluation of $\delta^{13}C$ chemostratigraphy for intrabasinal correlation: Vendian strata of northeast Siberia. GSA Bull. 108, 992–1003.

Perry, E.C., Feng, J., Hemzacek, J.M., 1984. Precambrian evaporites: preservation of sulfate in quartz pseudomorphs after gypsum. In: Proceedings of the 30th Annual Institute on Lake Superior Geology, p. 47.

Pettijohn, F.J., 1957. Paleocurrents of Lake Superior Precambrian quartzites. GSA Bull. 68, 469–480.

Pettijohn, F.J., 1943. Basal Huronian conglomerates of Menominee and Calumet Districts, Michigan. J. Geol. 51, 387–397.

Pickard, A.L., 2003. SHRIMP U–Pb zircon ages for the Palaeoproterozoic Kuruman Iron Formation, Northern Cape Province, South Africa: evidence for simultaneous BIF deposition on Kaapvaal and Pilbara Cratons. Precambrian Res. 125 (3/4), 275–315.

Pope, M.C., Grotzinger, J.P., 2003. Paleoproterozoic Stark Formation, Athapuscow Basin, Northwest Canada: record of cratonic-scale salinity crisis. J. Sed. Res. 73 (2), 280–295.

Prasad, N., Roscoe, S.M., 1996. Evidence of anoxic to oxic atmospheric change during 2.45–2.22 Ga from lower and upper sub-Huronian paleosols, Canada. Catena 27, 105–121.

Puffett, W.P., 1974. Geology of the Negaunee Quadrangle, Marquette County, Michigan. U.S. Geol. Surv. Prof. Paper 788, p. 53.

Rainbird, R.H., Nesbitt, H.W., Donaldson, J.A., 1990. Formation and diagenesis of a sub-Huronian saprolith: comparison with a modern weathering profile. J. Geol. 98, 801–822.

Rasmussen, B., Fletcher, I.R., Sheppard, S., 2005. Isotopic dating of the migration of a low-grade metamorphic front during orogenesis. Geology 33, 773–776.

Richardson Jr., E.S., 1949. Some lower Huronian stromatolites of northern Michigan. Fieldiana Geol. 10 (8), 47–62.

Riller, U., Schwerdtner, W.M., 1997. Mid-crustal deformation at the southern flank of the Sudbury Basin, central Ontario, Canada. GSA Bull. 109 (7), 841–854.

Riller, U., Schwerdtner, W.M., Halls, H.C., Card, K.D., 1999. Transpressive tectonism in the eastern Penokean orogen, Canada consequences for Proterozoic crustal kinematics and continental fragmentation. Precambrian Res. 93, 51–70.

Rousell, D.H., Long, D.G.F., 1998. Are outliers of the Huronian Supergroup preserved in structures associated with the collapse of the Sudbury impact crater? J. Geol. 106, 407–419.

Rust, B.R., Shields, M.J., 1986. Grant 189 The sedimentology and stratigraphy of the Bar River Formation (Huronian Supergroup) at Bay Finn, Lake Huron. In: Milne, V.G. (Ed.), Ontario Geological Survey Miscellaneous Paper 130, Geoscience Research Grant Program Summary of Research 1985–1986. Ministry of Northern Development and Mines, Mines and Minerals Division, pp. 16–23.

Salop, L.I., 1982. Geologic Development of the Earth in Precambrian. Nedra, Leningrad, 343 pp.

Schmidt, R.G., 1980. The Marquette Range Supergroup in the Gobebic Iron District, Michigan and Wisconsin. U.S. Geol. Surv. Bull. 1460, 96 pp.

Schneider, D.A., Bickford, M.E., Cannon, W.F., Schulz, K.J., Hamilton, M.A., 2002. Age of volcanic rocks and syndepositional iron formations, Marquette Range Supergroup: implications for the tectonic setting of Paleoproterozoic iron formations of the Lake Superior region. Can. J. Earth Sci. 39, 999–1012.

Schidlowski, M., Eichmann, R., Junge, C.E., 1975. Precambrian sedimentary carbonates: carbon and oxygen isotope geochemistry and implications for the terrestrial oxygen budget. Precambrian Res. 2, 1–69.

Schmitz, M.D., Bowring, S.A., Southwick, D.L., Boerboom, T.J., Wirth, K.R., 2006. High-precision U–Pb geochronology in the Minnesota River Valley subprovince and its bearing on the Neoarchean to Paleoproterozoic evolution of the southern Superior Province. GSA Bull. 118 (1/2), 82–93.

Severson, M.J., Zanko, L.M., Hauck, S.A., Oreskovich, J.A., 2003. Geology and sedex potential of Early Proterozoic rocks, East-Central Minnesota. Technical Report NRRI/TR-2003/35. Natural Resources Research Institute, University of Minnesota, Duluth, MN.

Sims, P.K., 1990. Geologic map of Precambrian rocks, Marenisco, Thayer, and Watersmeet 15-min Quadrangles, Gogebic and Ontonagon Counties, Michigan, and Vilas County, Wisconsin. U.S. Geol. Surv. Misc. Invest. Ser. Map I-2093.

Sims, P.K., Card, K.D., Lumbers, S.B., 1981. Evolution of Early Proterozoic basins of the Great Lakes Region. In: Campbell, F.H.A. (Ed.), Proterozoic Basins of Canada. Geological Survey of Canada, Paper 81-10, pp. 379–397.

Sims, P.K., Card, K.D., Morey, G.B., Peterman, Z.E., 1980. The Great Lakes tectonic zone—a major crustal structure in central North America. GSA Bull. 91, 690–698.

Sims, P.K., Peterman, Z.E., Prinz, W.C., Benedict, F.C., 1984. Geology, geochemistry, and age of Archean and Early Proterozoic rocks in the Marenisco-Watersmeet area, northern Michigan. U.S. Geol. Surv. Prof. Paper 1292-A, pp. A1–A41.

Smith, M.D., 2002. The timing and petrogenesis of the Creighton pluton, Ontario: an example of felsic magmatism associated with Matachewan igneous events. M.Sc. Thesis. The University of Alberta, Edmonton, 123 pp.

Smith, M.D., Heaman, L.M., 1999. Constraints on the timing of felsic magmatism associated with the Matachewan igneous events: preliminary results for the Creighton granite, Ontario. Geol. Ass. Canada, Min. Ass. Canada Joint Ann. Meeting Abstract 24, 119 pp.

Southwick, D.L., Morey, G.B., 1991. Tectonic imbrication and foredeep development in the Penokean orogen, east-central Minnesota—an interpretation based on regional geophysics and the results of test drilling. U.S. Geol. Surv. Bull. 1904-C, 17 pp.

Southwick, D.L., Day, W.C., 1983. Geology and petrology of Proterozoic mafic dikes, north-central Minnesota and western Ontario. Can. J. Earth Sci. 20, 622–638.

Southwick, D.L., Halls, H.C., 1987. Compositional characteristics of the Kenora-Kabetogama dyke swarm (Early Proterozoic), Minnesota and Ontario. Can. J. Earth Sci. 24, 2197–2205.

Sreenivas, B., Das Sharma, S., Kumar, B., Patil, D.J., Roy, A.B., Srinivasan, R., 2001. Positive $\delta^{13}$C excursion in carbonate and organic fractions from the Paleoproterozoic Aravalli Supergroup, Northwestern India. Precambrian Res. 106, 277–290.

Swart, Q.D., 1999. Carbonate rocks of the Paleoproterozoic Pretoria and Postmasburg Groups, Transvaal Supergroup. M.S. Thesis. Rand Africans University, Johannesburg, South Africa, 126 pp.

Taylor, G.L., 1972. Stratigraphy, sedimentology, and sulfide mineralization of the Kona Dolomite. Ph.D. Thesis. Michigan Technological Institute, Lansing, Michigan, 111 pp.

Tikhomirova, M., Makarikhin, V.V., 1993. Possible reasons for the $\delta^{13}$C anomaly of lower Proterozoic sedimentary carbonates. Terra Nova 5, 244–248.

Tucker, M.E., 1984. Calcitic, aragonitic and mixed calcitic-aragonitic ooids from the mid-Proterozoic Belt Supergroup, Montana. Sedimentology 31, 627–644.

Twenhofel, W.H., 1919. Pre-Cambrian and carboniferous algal deposits. Am. J. Sci., Fourth Ser. XLVIII (287), 339–352.

Tyler, S.A., Twenhofel, W.H., 1952. Sedimentation and stratigraphy of the Huronian of Upper Michigan. Am. J. Sci. 250, 8–27, 118–151.

Valley, J.W., 1986. Stable isotope geochemistry of metamorphic rocks. Rev. Miner. 16, 445–489.

Vallini, D.A., Cannon, W.F., Schulz, K.J., in press. Age constraints for Paleoproterozoic glaciation in the Lake Superior region: detrital zircon and hydrothermal xenotime ages for the Chocolay Group, Marquette Range Supergroup. Can. J. Earth Sci.

Vallini, D.A., Cannon, W.F., Schulz, K.J., 2005. New age data for the Chocolay Group, Marquette Range Supergroup: implications for the Paleoproterozoic evolution of the Lake Superior and Lake Huron regions [abstract], Institute on Lake Superior Geology Proceedings, 51th Annual Meeting, 51 (1), 64.

Vallini, D.A., McNaughton, N.J., Rasmussen, B., Fletcher, I., Griffin, B.J., 2003. Using xenotime U–Pb geochronology to unravel the history of Proterozoic sedimentary basins: a study in Western Australia and the Lake Superior Region [abs]. In: Proceedings of the 49th Annual Institute on Lake Superior Geology, vol. 49, Part 1, Iron Mountain, MI, pp. 79–80.

van Breemen, O., Bostock, H.H., 1994. Age of emplacement of Thoa metagabbro, western margin of Rae Province, Northwest Territories: initiation of rifting prior to Taltson magmatism? Geological Survey of Canada, Paper 1994-F, Radiogenic age and isotopic studies: report 8, pp. 61–68.

Van Hise, C.R., Bayley, W.S., 1897. The Marquette iron-bearing district of Michigan, including a chapter on the Republic Trough by H.L. Smyth. U.S. Geol. Surv. Mon. 28, 608.

Veizer, J., 1983. Chemical diagenesis of carbonates: theory and application of trace element technique, Stable isotopes in Sedimentary Geology. SEPM Short Course 10, Dallas, pp. 3-1–3-100.

Veizer, J., Clayton, R.N., Hinton, R.W., 1992. Geochemistry of Precambrian carbonates. IV. Early Paleoproterozoic ($2.25 \pm 0.25$ Ga) seawater. Geochim. Cosmochim. Acta 56, 875–885.

Velikoslavinsky, S.D., Kotov, A.B., Sal'nikova, E.B., Glebovitsky, V.A., Kovach, V.P., Zagarnaya, N.Y., Belyaevsky, N.A., Yakovleva, S.Z., Fedoseenko, A.M., 2003. The U–Pb age of the Fedorov Sequence of the Aldan granulite-gneiss megacomplex, the Aldan Shield. Doklady Earth Sci. 393 (8), 1151–1155.

Vinogradov, V.I., Reimer, T.O., Leites, A.M., Smelov, S.B., 1976. The oldest sulfates in the Archean Formations of the South African and the Aldan Shields, and the evolution of the Earth's oxygen atmosphere. Lithol. Miner. Resour. 11 (4), 407–420.

Walraven, F., 1997. Geochronology of the Rooiberg Group, Transvaal Supergroup, South Africa. Econ. Geol. Res. Unit, University of the Witwatersrand, Inf. Circ. 316, Johannesburg, South Africa, 21 pp.

Wickham, S.M., Peters, M.T., 1993. High $\delta^{13}$C Neoproterozoic carbonate rocks in western North America. Geology 21, 165–168.

Wier, K.L., 1967. Geology of the Kelso Junction Quadrangle Iron County, Michigan. U.S. Geol. Surv. Bull. 1226, 47.

Wohlabaugh, N., 1980. Petrology of the Big Cusp Algal Dolomite; An informal member of the Kona Dolomite, Marquette, Michigan. M.Sc. Thesis. Bowling Green State University, 164 pp.

Wohlabaugh, N., Mancuso, J.J., 1990. Depositional and diagenetic history of the Big Cusp Algal Dolomite, Kona Formation, Marquette Range, Michigan. The Compass 67 (2), 84–93.

Wood, J., 1979. No. 18 Regional geology of the Cobalt Embayment, District of Sudbury, Nipissing, and Timiskaming: Summary of fieldwork. Ontario Geological Survey, Misc. paper 90, pp. 79–81.

Wood, J., 1973. Stratigraphy and depositional environments of upper Huronian rocks of the Rawhide Lake–Flack Lake area, Ontario. In: Young, G.M. (Ed.), Huronian Stratigraphy and Sedimentation. Geol. Assn. Can. Spec. Paper 12, pp. 73–95.

Young, G.M., 2004. Earth's earliest glaciations: tectonic setting and stratigraphic context of Paleoproterozoic glaciogenic deposits. In: Jenkins, G.S., McMenamin, M.A.S., McKay, C.P., Sohl, L. (Eds.), The Extreme Proterozoic: Geology, Geochemistry, and Climate. AGU Geophysical Monograph Series 146, pp. 161–181.

Young, G.M., 2002. Stratigraphic and tectonic settings of Proterozoic glaciogenic rocks and banded iron-formations: relevance to the snowball Earth debate. J. Afr. Earth Sci. 35, 451–466.

Young, G.M., Long, D.G.F., Fedo, C.M., Nesbitt, H.W., 2001. Paleoproterozoic Huronian basin: product of a Wilson cycle punctuated by glaciations and a meteorite impact. Sed. Geol. 141/142, 233–254.

Young, G.M., 1991. Stratigraphy, sedimentology and tectonic setting of the Huronian Supergroup. In: Proceedings of the Joint Annual Meeting, Toronto'91, Field trip B5: Guidebook, Geological Association of Canada, Mineralogical Association of Canada, Society of Economic Geologists, 34 pp.

Young, G.M., 1988. Proterozoic plate tectonics, glaciation and iron-formations. Sediment. Geol. 58, 127–144.

Young, G.M., 1983. Tectono-sedimentary history of Early Proterozoic rocks of the northern Great Lakes region. In: Medaris Jr., L.G. (Ed.), Early Proterozoic Geology of the Great Lake Region. Geol. Soc. Am. Mem. 160, pp. 15–32.

Yudovich, Y.Y., Makarikhin, V.V., Medvedev, P.V., Sukhanov, N.V., 1990. Carbon isotope anomalies in carbonates of Karelian Series. Geochemistry (7), 972–978.

Zolnai, A.I., Price, R.A., Helmstaedt, H., 1984. Regional cross section of the Southern Province adjacent to Lake Huron, Ontario: implications for the tectonic significance of the Murray Fault Zone. Can. J. Earth Sci. 21, 447–456.

Zolotarev, A.A., Efremov, G.M., Brotigam, B., Ivanova, T.V., 1989. Isotopic composition of sulfur in sulfates of Seligdar apatite deposit (Central Aldan). Geokhimiya (11), 1656–1659.